Geol. Paläont. Mitt. Innsbruck, ISSN 0378–6870, Band 26, S. 21–45, 2003

5TH WORKSHOP OF ALPINE GEOLOGICAL STUDIES FIELD TRIP GUIDE E4 ALPINE METAMORPHISM IN THE SCHNEEBERG COMPLEX AND NEIGHBOURING UNITS (IMMEDIATE VICINITY OF OBERGURGL)

Jürgen Konzett, Georg Hoinkes & Peter Tropper

With 20 figures

I. Ötztal-Stubai Crystalline Complex and Schneeberg Complex

1. Geology

The Ötztal-Stubai Crystalline Complex (ÖSCC) is part of the Austroalpine nappe system which was emplaced on the Penninic units during the Alpine Orogeny (Fig. 1). The ÖSCB shows numerous similarities to the Silvretta Nappe in terms of petrologic evolution and structures, indicating an originally similar tectonic position with subsequent dissection by Tertiary updoming of the Engadine Window.

1.1. Boundaries of the ÖSCB

The E border of the ÖSCC towards the Tauern Window is formed by the N-S trending Brenner line which is a W-dipping detachment fault with an

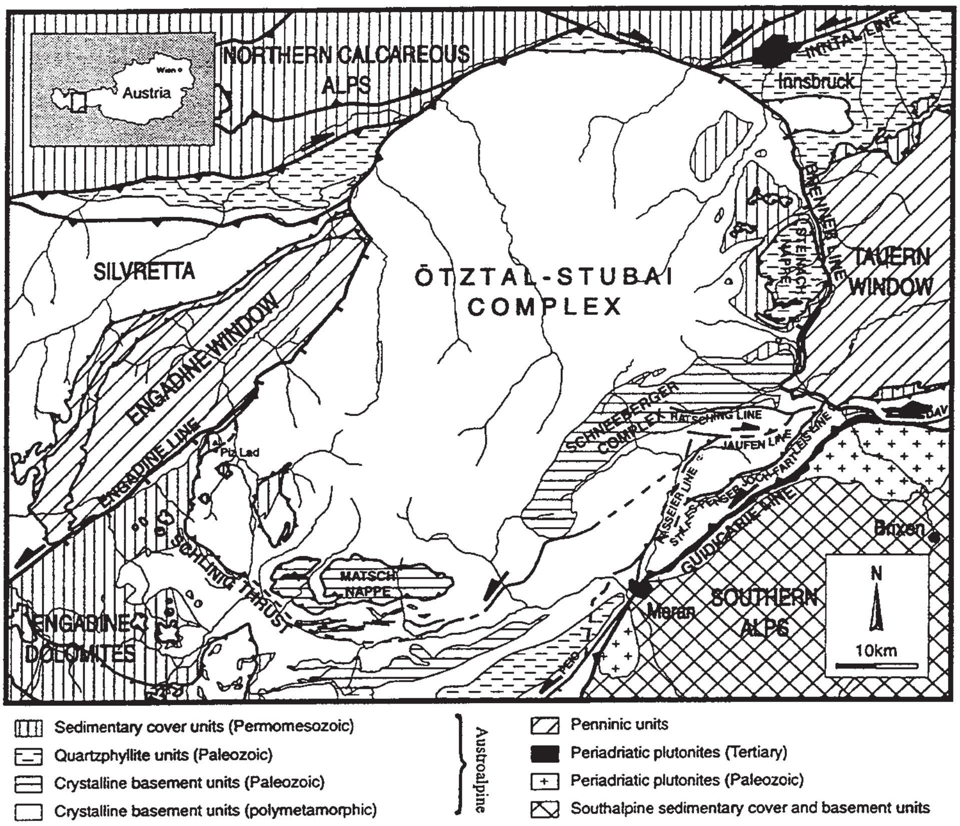

Fig. 1: Simplified geological map of the ÖSCC complex and adjacent areas [modified after Thöni (1981), taken from Elias (1998)]

estimated minimum lateral displacement of 15-26 km (Selverstone et al. 1995; Fügenschuh 1995). The N border of the ÖSCC towards the Northern Calcareous Alps is formed by the Inntal line, a sinistral strike-slip fault. The W border towards the Engadine Window is formed by the Engadine line (Trümpy 1977). Movements along this line are strike-slip with respect to the Periadriatic line or oblique slip (Schmidt & Haas 1989). The S border is tectonically more complex and in the SW formed by the Schlinig thrust along which the ÖSCC has overridden the Austroalpine Sesvenna nappe. Further to the E the Schlinig line shows a transition into a km-wide shear zone and at the SE border of the ÖSCB it is not possible to define the continuation of the Schlinig line. A possible continuation, however, is represented by the Passeier and Jaufen lines (Fig. 1, see also Elias (1998) for a more comprehensive discussion).

1.2. Lithology and structures

The ÖSCC consists of polymetamorphic basement units of medium- to high-grade gneisses of pelitic to psammitic origin with intercalations of micaschists, quartzites, orthogneisses, amphibolites, eclogites and rare marbles.

The Schneeberg Complex (SC) represents a remnant of a Paleozoic metasedimentray cover with normal stratigraphic relations and consists of several E-W trending synclines overturned to the S with a strikingly different lithology compared to the adjacent ÖSCC rocks (cf. Frank et al. 1987) The SC rocks are monometamorphic and deeply folded into the underlying ÖSCC. The strike of the fold structures changes in W-E direction from NNE-SSW to ENE-WSW. To the north, the main syncline („Schneeberger Hauptmulde") is characterized by a broad central zone of garnet-micaschists („monotone Serie") and small marginal zones of amphibole-bearing rocks, quartzites and marbles („bunte Randserie"). To the SW, two smaller synclines – the Schrottner- and Seeberspitz-synclines - are folded into micaschist country-rocks. Along the southern margin of the SC, a zone of crystalline rocks with striking lithological similarities to the SC occurs. This zone is called „Laas Series" and forms a third syncline (Lodner Syncline) along the SW border of the SC (Fig. 2). In spite of its similarities to the SC rocks, the Laas Series has to be assigned to the ÖSCC s.s. due to its polymetamorphic evolution (Konzett 1990).

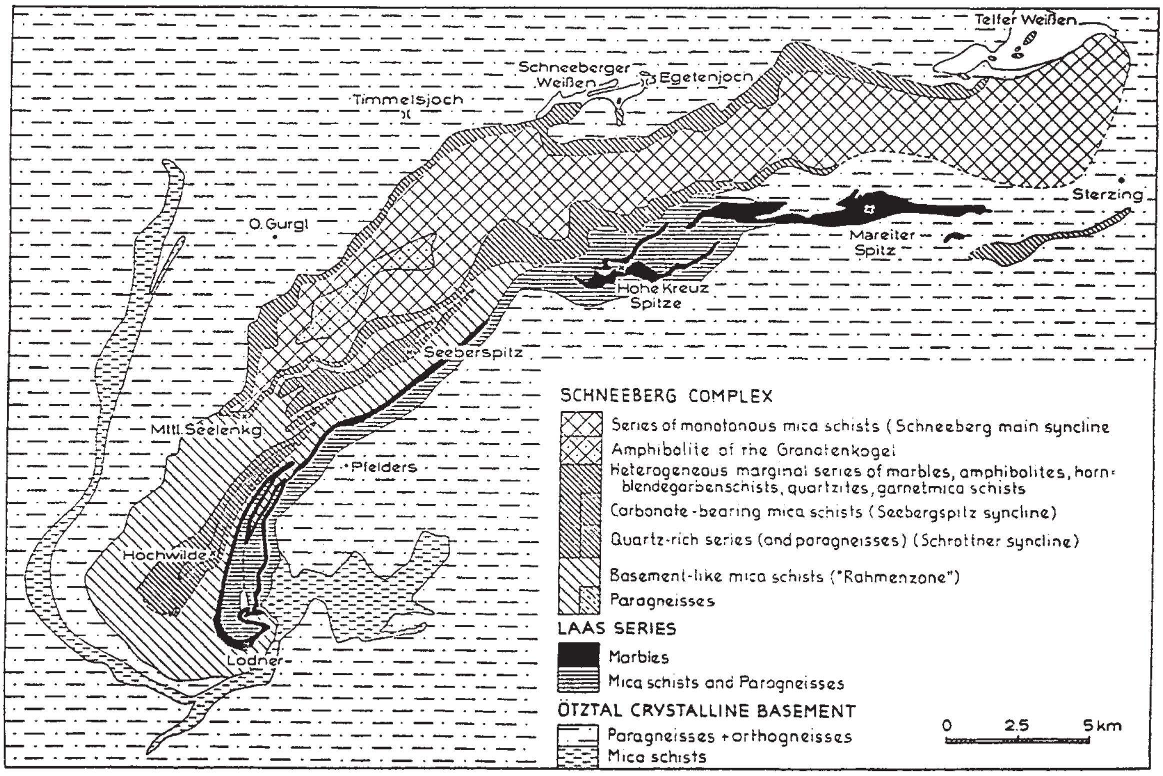

Fig. 2: Simplified sketch of the Schneeberg Complex and surrounding rocks (from Hoinkes 1987)

Relics of the sedimentary Permomesozoic cover of the ÖSCC are preserved along the western side of the Brenner line ("Brenner Mesozoic") and at the northern margin of the SC ("Telfer Weisse", "Schneeberger Weisse"). These parautochthonous cover sequences show only locally developed tectonic contacts (Fügenschuh & Rockenschaub 1993).

Rapid exhumation of the ÖSCC during late Cretaceous to early Tertiary let to a thrusting of upper Austroalpine units ("Blaser Decke", "Steinacher Decke") on top of the Permomesozoic sediments (Fügenschuh et al. 2000) (Fig. 1).

Different tectonic styles are prevalent in the northern and southern part of the ÖSCC: The northern part is characterized by E-W trending fold axes and an E-W orientation of intercalated orthogneisses. In the southern part of the ÖSCC, no such preferred orientation can be observed. By contrast, km-scale folds with steeply dipping fold axes ("Schlingentektonik" or vortex tectonics) and a partly intense mm-scale folding are the characteristic structural features that can be found in both the ÖSCC and SC. The age of the "Schlingentektonik" is assumed to be – at least in part – Eo-Alpine (Schmid & Haas 1989)

The structural evolution of the ÖSCC is complex and has been subject of several studies (van Gool et al. 1987; Fügenschuh 1995; Fügenschuh et al. 2000; Stöckli 1995). A comparison of structures/deforma-

van Gool et al. (1987)[1)]	Fügenschuh (1995)[2)]	Stöckli (1995)[3)]	Age	Structures
pre-D1			?	[1)] Isoclinally folding of sedimentary layering
D1			Variscan	[1)] Finely spaced schistosity and crenulation cleavage with tight to isoclinal folds.
D2			Variscan	[1)] Widely spaced schistosity and crenulation cleavage with folds of varying morphology.
D3			Variscan? *)	[1)] Structures with steeply N-dipping axial plane, striking approximately E-W
D4 **)	pre-D1		Late Cretaceous	[1)] E-W to WNW-ESE trending folds and generally subhorizontal shear zones. [2)] Top-to-the-W directed shear movements.
	D1	$D1_{AA}$ ***)	Late Cretaceous	[2)] WNW-ESE stretching lineations and top-to the-SSE to SE directed movements. [3)] NW-SE stretching lineations shallowly plunging to the SE and top-to-the SE directed movements.
	D2		Paleogene	[2)] NE-SW oriented fold axes which are related to NW-SE shortening.
		$D2_{AA}$	Early Oligocene	[3)] Subhorizontal ENE-WSW trending stretching lineations and left-lateral mylonitization.
	D3	$D3_{AA}$	Miocene	[2)] Steeply dipping normal faults with varying amount of strike-slip components compatible with N-S shortening and E-W extension. [3)] Subhorizontal stretching lineations which generally plunge shallowly to the WSW and right-lateral mylonitization.
		$D4_{AA}$ ****)	Miocene	[3)] E-W trending fold axes and axial planes dipping shallowly to the N which are related to south-vergent backthrusting. SSE-directed backthrusting is correlated with asymmetric S-vergent folding in the cover sequences.
		$D5_{PT}$	Miocene	[3)] E-dipping normal faults with variable dextral components and subordinated NNE-SSW trending sinistral strike-slip faults in the cover sequences.

Table 1: Structural evolution of the southern and eastern parts of the ÖSCC and the southeastern adjacent Austroalpine areas based on the compiled data of van Gool et al. (1987), Fügenschuh (1995) and Stöckli (1995); *) The age of D3 structures is still a matter of discussion; **) D4 structures of van Gool et al. (1987) encompass Cretaceous as well as Tertiary structures;***) Stöckli (1995) distinguishes deformation phases in the basement (D_{AA}) and Permotriassic cover (D_{PT}) units which not always correlate internally in time. D_{1AA} also includes top-to-the W directed movements which correlate to pre-D1 of Fügenschuh (1995) (see also Stöckli 1995); ****) Stöckli (1995) separates two phases in the cover units which are regarded as continuation of the same progressive process of backfolding and backthrusting.

tion phases distinguished by these authors is given in Table 1.

2. Metamorphic evolution of the ÖSCC

At least three metamorphic events can be traced in the ÖSCC rocks whose characteristics are briefly described below:

2.1. The Caledonian event

This event is recorded by migmatites developed in biotite-plagioclase gneisses of the central ÖSCC (e.g. Winnebach migmatite); P-T conditions of 660-685°C at ≥ 4 kbar (upper amphibolite/lower granulite facies); age of metamorphism 420 – 460 Ma (Chowanetz 1991, Schweigl 1995).

2.2. The Variscian event

This event reaches conditions of eclogite- to amphibolite facies in the ÖSCC

- eclogite facies: recorded in metabasic (gabbroic/basaltic) and meta-ultrabasic rocks of the central ÖSCC; P-T conditions of eclogite facies: around 27 kbar/730°C; age of metamorphism 360-350 Ma (Miller & Thöni 1995).
- amphibolite facies: recorded in widespread metapelites by Al_2SiO_5 assemblages ± staurolite; regional distribution of the Al_2SiO_5 modifications: Sillimanite: central ÖSCC; kyanite: northern and southern ÖSCC; andalusite: small area within sillimanite zone where all three modifications may occur together (Fig. 3); conditions of amphibolite-facies: around 650°C and 7 kbar (Hoinkes & Thöni 1993); age of metamorphism 343-331 Ma (Thöni 1993).

2.3. The Eo-Alpine event

The P-T conditions of this event increase from sub-greenschist conditions in the NE to epidote-amphibolite/eclogite conditions in the SW. This event leads to the neoformation of Eo-Alpine assemblages along NE-SW trending isogrades (e.g. zone early Alpine chloritoid; Purtscheller 1978). Where Eo-Alpine conditions are lower-grade than Variscian

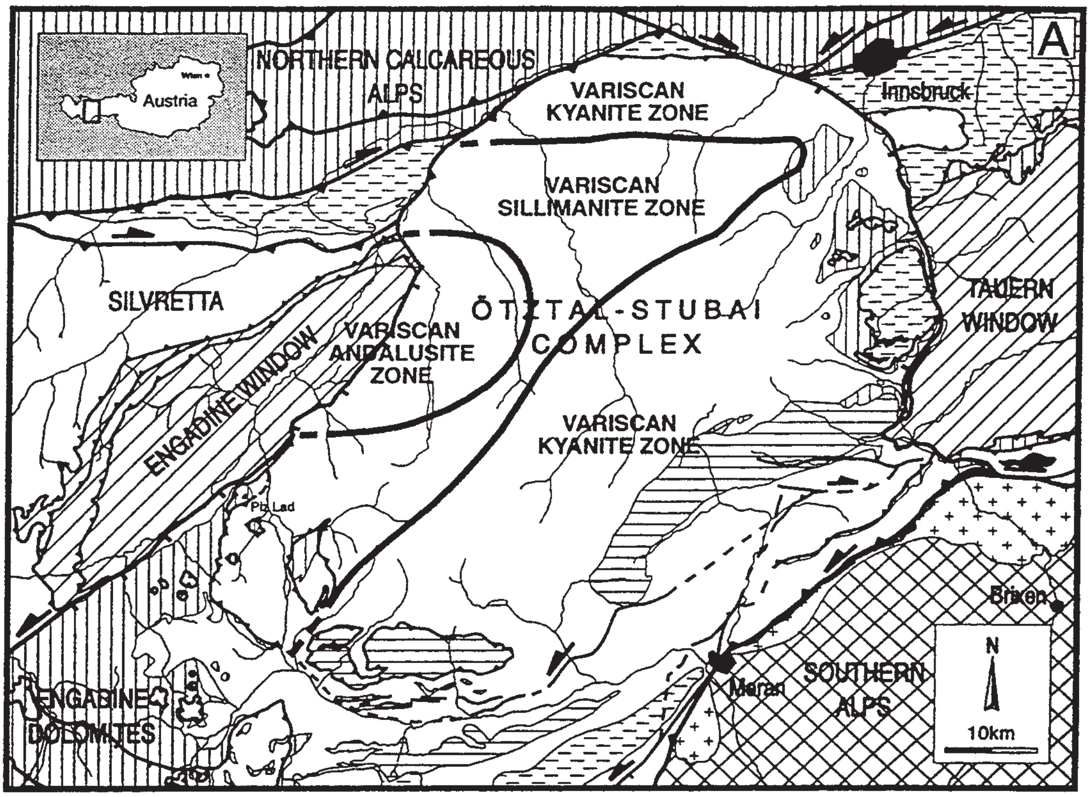

Fig. 3: Sketch of distribution of Variscian Al2SiO5 assemblages in metapelites of the ÖSCC (taken from Elias 1998); figure caption as for Fig. 1.

conditions, a retrogressive breakdown of Variscan assemblages (e.g. staurolite ⇒ chloritoid; staurolite ⇒ paragonite + chlorite) can be observed.

Peak metamorphic conditions of the Eo-Alpine event are reached in the southwestern ÖSCC in an area comprising parts of the SC and the underlying basement. Rocks in this area record (epidote-)amphibolite to eclogite facies conditions (Konzett & Hoinkes 1996, Hoinkes et al. 1991, Habler et al. 2001, Exner et al. 2001). The area of max. Eo-Alpine P-T conditions is characterized by the neo-formation of staurolite and kyanite in metapelites. The characteristic assemblage in metapelites is Ga + Bio + Mu + Plag + Qz ± Pa ± Sta ± Ky.

- epidote-amphibolite facies: recorded in the monometamorpic SC rocks; P-T conditions around 600°C and 8-10 kbar
- eclogite facies: recorded in basic eclogites and orthogneisses of the polymetamorpic basement rocks immediately S of the SC; P-T conditions 500–550°C and ≥ 11-12 kbar; the T-maximum along the P-T loop followed by the eclogites and their contryrocks is represented by amphibolite facies conditions with 600-650°C and 5-6 kbar.

The Eo-Alpine metamorphic zoning is truncated by the Passeier-Jaufen line. S of this line subgreenschist to lower greenschist facies conditions are recorded by both basement and cover units.

The Eo-Alpine overprint leads to a continuous rejuvenation of Variscian Rb-Sr and K-Ar mica cooling ages in a regional pattern following the Eo-Alpine mineral isogrades (Fig. 3): In the northwestern ÖSCC the very weak Eo-Alpine overprint preserves Variscian mica ages in the range 200-300 Ma; increasing Eo-Alpine conditions are indicated by a decrease in ages towards SW with a complete reset to ages in the range 80-100 Ma in the area of maximum Eoapline P-T conditions (Elias 1998 and references therein).

3. Cooling and exhumation of the ÖSCC

Cooling of the ÖSCC after the peak of Eo-Alpine metamorphism started around 90-100 Ma and ended some 30 Ma later at near surface temperatures. According to Elias (1998) cooling of the ÖSCC was uneven with periods of rapid cooling around

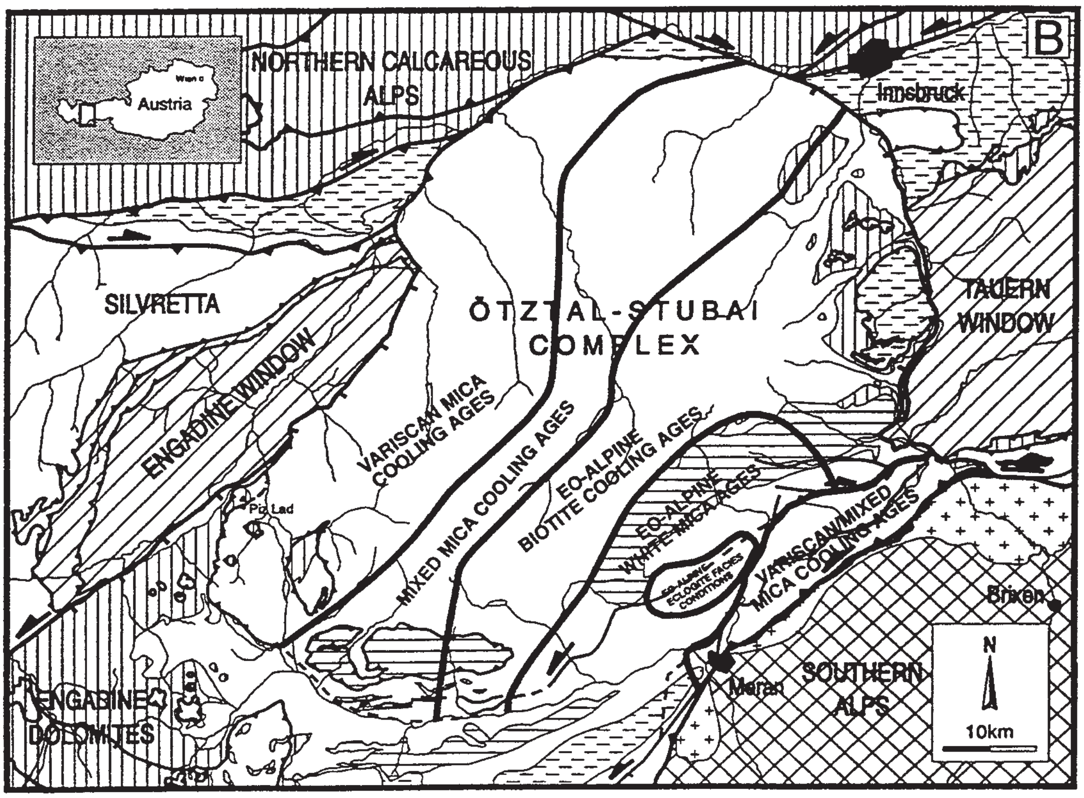

Fig. 4: Sketch of mica cooling age patterns in the ÖSCC resulting from Eo-Alpine overprint of Variscian assemblages (Taken from Elias 1998); figure caption as for Fig. 1.

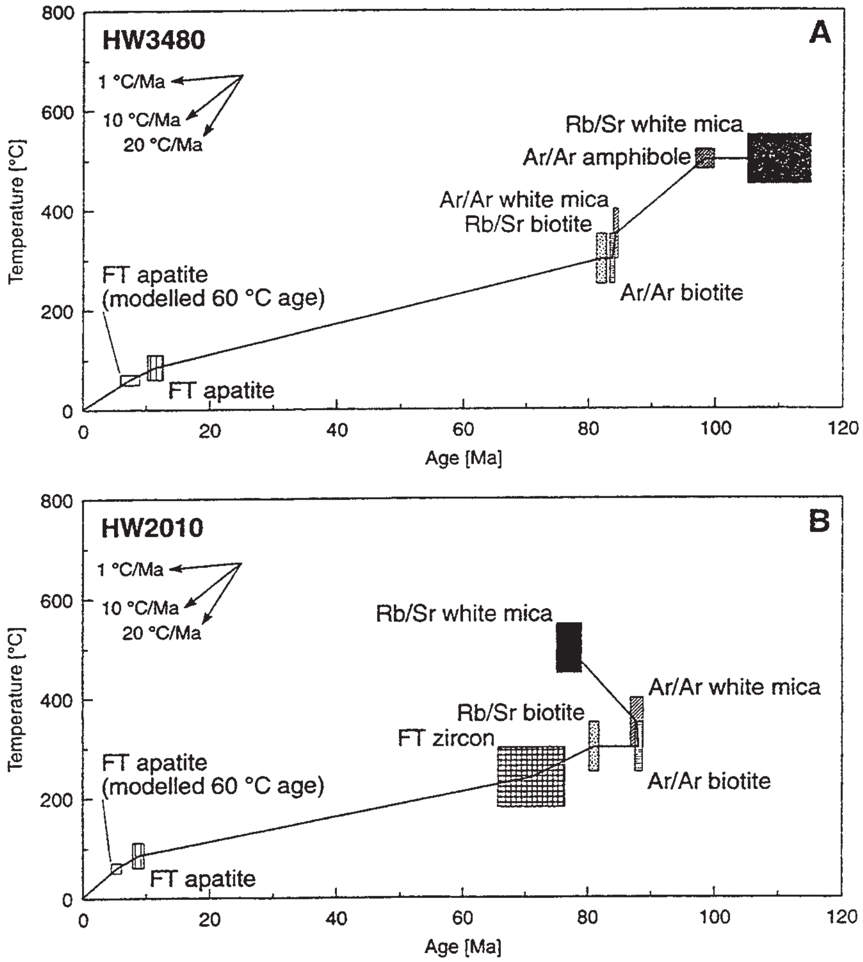

Fig. 5: Cooling paths of a vertical profile in the SW part of the SC reflecting max. possible differences in altitude of around 1500 m; (A) data of the present peak plain of ca. 3500 m which are interpreted to reveal a minimum age of the Eo-Alpine thermal peak; (B) age data of the lowest sample altitude in the profile of around 2000 m confirming an Eo-Alpine period of rapid cooling around 80 Ma. (from Elias 1998)

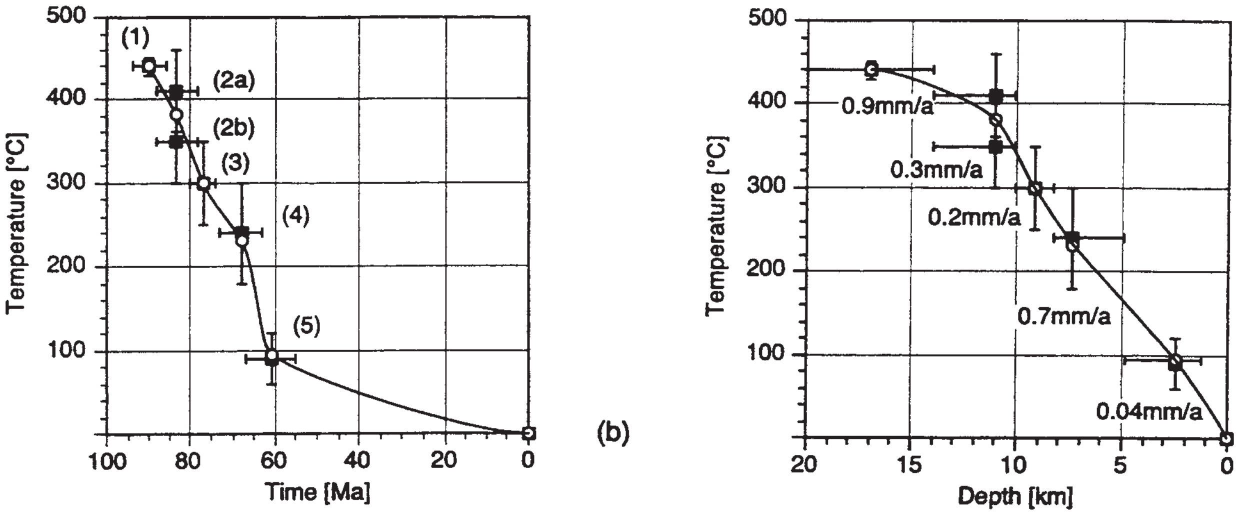

Fig. 6: Modelled (a) temperature-time and (b) temperature-depth paths for the northeastern ÖSCC using one-dimensional thermal modeling (from Fügenschuh et al. 2000)

100, 80, and 6-8 Ma and intermittent periods of insignificant cooling (Fig. 5). For the Eastern part of the ÖSCC, Fügenschuh (2000) found evidence for late Cretaceous/early Tertiary exhumation due to low-angle normal faulting. His results indicate decreasing exhumation rates from around 1 mm/a for late Cretaceous/early Tertiary to 0.7–0.2 mm/a (Fig. 6). According to Fügenschuh (2000) the pattern of Eo-Alpine metamorphic assemblages directly reflects the geometry and kinematics of this late Cretaceous/early Tertiary exhumation due to low-angle normal faulting.

4. References

Chowanetz, E., 1991. Strukturelle und geologische Argumente für eine altpaläozoische Anatexis im Winnebachmigmatit (Ötztal/Tirol, Österreich). Mitteilungen der österreichischen Geologie- und Bergbaustudenten **37**, 15–35.

Elias, J., 1998. The thermal history of the Ötztal-Stubai Complex (Tyrol, Austria/Italy) in the light of the lateral extrusion model. Tübinger Geowissenschaftliche Arbeiten **42**, 172 pp.

Exner, U., Fussein, F., Grasemann, B., Habler, G., Linner, M., Sölva, H., Thiede, R. & Thöni, M., 2001 Cretaceous Eclogite-Facies Metamorphism in the Eastern Alps: New Insights, Data and Correlations from an Interdisciplinary Study. Journal of Conference Abstracts **6**, 387.

Frank, W., Hoinkes, G., Purtscheller, F. & Thöni, M., 1987. The Austroalpine unit west of the Hohe Tauern: The Ötztal-Stubai Complex as an example for the Eo-Alpine Metamorphic evolution. In: Flügel, H.W. & Faupl, P. (eds.) Geodynamics of the Eastern Alps, Deuticke, Vienna 1987, pp. 179–225.

Fügenschuh, B., 1995. Thermal and kinematic history of the Brenner area (Eastern Alps, Tyrol). Unpublished Ph.D. Thesis, ETH-Zürich, 165 pp.

Fügenschuh, B. & Rockenschaub, M., 1993. Deformations in the hangingwall of the Brenner-fault zone. Terra Abstracts **5**, p. 165.

Fügenschuh, B., Mancktelow, N.S. & Seward, D., 2000. Cretaceous to Neogene cooling and exhumation history of the Oetztal-Stubai basement complex, eastern Alps: A structural and fission track study. Tectonics **19**, 905–918.

Habler, G., Linner, M., Thiede, R. & Thöni, M., 2001. Eo-Alpine Andalusite in the Schneeberg Complex (Eastern Alps, Italy/Austria): Constraining the P-T-t-D Path during Cretaceous Metamorphism. Journal of Conference Abstracts **6**, 340.

Hoinkes, G. & Thöni, M., 1993. Evolution of the Ötztal-Stubai, Scarl-Campo and Ulten basement units. In: Von Raumer, J.F. & Neubauer, J.F. (eds.) Premesozoic geology in the Alps, pp 485–494.

Hoinkes, G., Kostner, A. & Thöni, M., 1991. Petrologic constraints for Eo-Alpine eclogite facies metamorphism in the Austroalpine Ötztal basement. Mineralogy and Petrology **43**, 237–254.

Konzett, J., 1990. Petrologie des zentralen Schneeberger Zugs und des südlich angrenzenden Kristallins im Bereich der Hohen Kreuzspitze, Passeiertal, Südtirol. Unpublished diploma thesis, 237 pp.

Konzett, J. & Hoinkes, G., 1996. Paragonite-hornblende assemblages and petrological significance: an example from the Austroalpine Schneeberg Complex, Southern Tyrol, Italy. Journal of Metamorphic Geology **14**, 85–101.

Miller , C. & Thöni, M., 1995. origin of eclogites from the Austroalpine Ötztal basement (Tyrol, Austria): geochemistry and Sm-Nd vs. Rb-Sr isotope systematics. Chemical Geology **122**, 199–225.

Schmid, S. & Haas, R., 1989. Transition from near-surface thrusting to intrabasement decollment, Schlinig thrust, Eastern Alps. Tectonics **8**, 697–718.

Schweigl, J., 1995. Neue geochronologische und isotopengeologische Daten zur voralpidischen Entwicklungsgeschichte im Ötztalkristallin (Ostalpen). Jahrbuch der geologischen Bundesanstalt **138**, 131–149.

Selverstone, J., Axen, G. & Bartley, J., 1995. Kinematic tests of dynamic models for footwall unroofing during extension in the Eastern Alps. In: Schmid, S., Froizheim, N., Heilbronner, R., Stünitz, H. & Frey, M. (eds.) Second Workshop on Alpine Geology, Basel, pp. 56–58.

Stöckli, D., 1995. Tectonics SW of the Tauern Window (Mauls area, South Tyrol). Southern continuation of the Brenner Fault Zone and its interaction with other large fault structures. Unpublished diploma thesis, ETH Zürich, 270 pp.

Thöni, M., 1993. Neue Isotopendaten zur voralpidischen Geschichte des Ötztalkristallins. Arbeitstagung der geologischen Bundesanstalt, 10–112.

Trümpy, R., 1977. The Engadine Line: a sinistrl wrench fault in the Central Alps. Memoirs of the Geological Society of China **2**, 1–17.

Van Gool, J.A.M., Kemme, M.M.J. & Schreurs, G.M.M.F., 1987. Structural investigations along an E-W cross-section in the southern Ötztal Alps. Flügel, H.W. & Faupl, P. (eds.) Geodynamics of the Eastern Alps, Deuticke, Vienna 1987, 214–222.

Topographic and geological maps

Freytag & Berndt Wanderkarte WKS 8 1: 50.000 Passeier-Timmelsjoch-Jaufen
Österreichische Karte 1 : 50.000: Blatt 174 Timmelsjoch
Carta Geologica d'Italia, Foglio IV, Merano (IIEd., Salerno), 1 : 100.000, (1970)

II. Field Stops

Stop No. 1: garnet-biotite-plagioclase-staurolite gneisses of the Ötztal-Stubai Crystalline Complex N of the Schneeberg Complex

Locality: Timmelsjoch; altitude 2474 m; Austrian-Italian border

The rocks outcropping in the immediate vicinity of the customs building are gneisses of the ÖSCC that form the northern border of the SC. The gneisses were affected by both Variscian and Eo-Alpine metamorphism: The Varisician metamorphism reached conditions of the amphibolite facies which led to the formation of an assemblage plagioclase + biotite + muscovite + garnet + quartz ± staurolite ± kyanite. The subsequent Eo-Alpine event in this area reached P-T conditions slightly below the stability of staurolite. This caused a retrogressive breakdown of staurolite according to a reaction (simplified in the NAMSH system):
staurolite + albite + H_2O ⇒ paragonite + chlorite + quartz

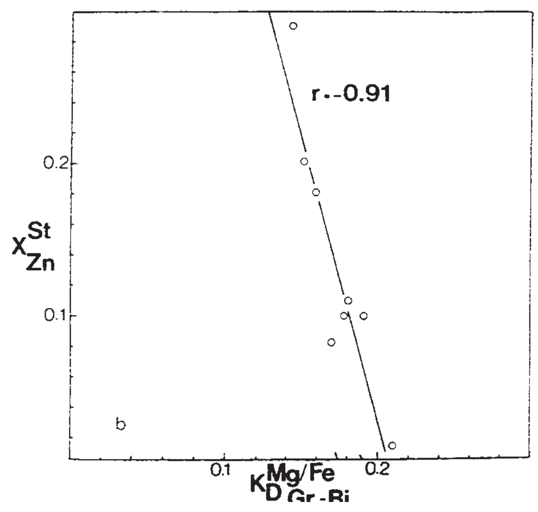

Fig. 1: Plot of Zn-concentration in staurolite vs K_D for Fe-Mg exchange between coexisting garnet and biotite for garnet-staurolite micaschists of the SC (from Hoinkes 1981)

This reaction caused the formation of mica+chlorite+quartz-pseudomorphs after lath-shaped staurolite crystals that may reach several cm in length and can be found on cleavage planes. P-T-conditions sufficient for Eo-Alpine staurolite formation, however, were reached within the northernmost part of the SC. The first Eo-Alpine staurolites that appear in micaschists just within the SC are rich in Zn with up to 5.6 wt% ZnO and are stabilized towards lower temperatures by Zn as evidenced by the negative correlation between $KD^{Fe-Mg}{}_{ga-bio}$ and X_{Zn} in staurolite (Fig. 1) (Hoinkes 1981).

Stop No. 2: Rocks of the Schneeberg Complex and the underlying basement of the Ötztal-Stubai Crystalline Complex – northern border of the Schneeberg Complex

Locality: Timmelsjoch road on the Italian side; altitude 2200 m; second 180°-road turn to the right.

Along the roadside the northern border of the main syncline of the Schneeberg Complex towards the underlying Ötztal-Stubai-Crystalline Complex is exposed. At this location the distinction between both units is unambigous due to the difference in lithologies:

Rocks of the ÖSCC:
- monotonous gneisses with abundant small (≤ 1 mm) garnet and biotite

Rocks of the SC:
- garnet-micaschists with large (0.5 to > 1cm) garnets
- amphibole-bearing rocks with large (≥ 1cm) amphiboles
  quartzites

The SC rocks exposed belong to the marginal series ("bunte Randserie") of intercalated garnet-micaschsists, amphibolites, hornblende garbenschists, marbles and quartzites that delimit the main syncline of the SC. Further downhill, rocks of the central SC main syncline are encountered that are charac-

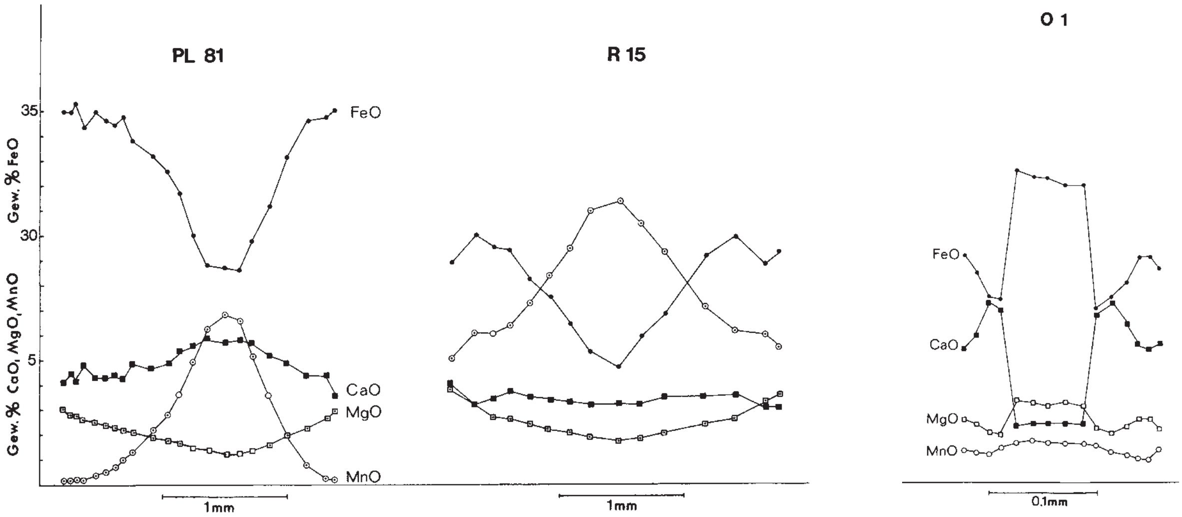

Fig. 1: Chemical zoning patterns of garnets from the SC (samples PL81, R15) and ÖSCC (sample O1)

terized by rather monotonous garnet-micaschists ("monotone Serie").

The SC-ÖSCC boundary is located a few meters uphill from a quartzite band that can unambigously be assigned to the SC. The actual boundary lies within several meters of gneisses containing small garnets and cannot unambigously be localized in the field. A definite criterion for the distinction between SC and ÖSCC rocks, however, is the zoning pattern of garnets (Fig. 1).

SC rocks are monometamorphic ⇒ garnets show continuous bell-shaped zoning patterns

ÖSCC rocks are polymetamorphic ⇒ garnets show discontinuous chemical zoning

Hoinkes, G., 1981. Mineralreaktionen und Metamorphosebedingungen in Metapeliten des westlichen Schneebergerzuges und des angrenzenden Altkristallins. Tschermaks Mineralogische und Petrographische Mitteilungen **28**, 31–54.

Stop No. 3: Rocks of the Schneeberg Complex – garnet-micaschists of the SC main syncline ("monotone Serie")

Locality: Timmelsjoch road on the Italian side; hamlet of Saltnuss (1680 m)

From Saltnuss towards Timmeljoch garnet-micaschists of the SC main syncline are exposed along the road. The typical assemblage encountered in these micaschists is
garnet + biotite + muscovite + paragonite + plagioclase + quartz ± kyanite ± staurolite

Kyanite formation can be attributed to a reaction
paragonite + quartz = kyanite + albite + H_2O
that *locally* proceeded at temperatures of 570-580°C due to a reduction of a(H_2O) in the fluid phase and/or a reduction a(albite) in plagioclase. The assemblage paragonite + quartz is generally stable in SC rocks which indicates that (P)-T conditions for paragonite-breakdown in the pure system NASH were not yet reached in this area.

For staurolite formation, textures indicate two possible reactions (Proyer 1989)
paragonite + garnet + quartz = staurolite + plagioclase + H_2O
paragonite + biotite + garnet + quartz = staurolite + plagioclase + muscovite + H_2O

The formation of abundant staurolite in micaschists within the ÖSCC South of the SC (e.g. Laaser Serie) is due to a discontinuous reaction
garnet + chlorite + muscovite = staurolite + biotite + quartz + H_2O
which only proceeds at peak metamorphic conditions of the Eo-Alpine event (570-580°C) (Hoinkes 1981). Most recently, Habler et al. (2001) reported andalusite from staurolite-garnet-micaschists of the SC main

syncline formed during the retrogressive stage of the Eo-Alpine event at temperatures ≥ 540°C.

Habler, G., Linner, M., Thiede, R. & Thöni, M., 2001. Eo-Alpine Andalusite in the Schneeberg Complex (Eastern Alps, Italy/Austria): Constraining the P-T-t-D Path during Cretaceous Metamorphism. Journal of Conference Abstracts 6, 340.

Hoinkes, G., 1981. Mineralreaktionen und Metamorphosebedingungen in Metapeliten des westlichen Schneebergerzuges und des angrenzenden Altkristallins. Tschermaks Mineralogische und Petrographische Mitteilungen 28, 31–54.

Proyer, A., 1989. Petrologie der Rahmengesteine der Pb-Zn Lagerstätte Schneeberg, Südtirol. Unpublished Diploma thesis, Innsbruck, 103 pp.

Stop No. 4: Eclogites and eclogite-amphibolites of the southern Ötztal-Stubai Crystalline Complex

Locality: outcrop of a few m in size along a forest track that branches of the main road from St. Leonhard i. Passeier to Meran approximately 3 km S of St. Martin

Description of eclogite assemblages taken from: Hoinkes, G., Kostner, A. and Thöni, M. (1991) Petrologic Constraints for Eo-Alpine Eclogite Facies Metamorphism in the Austroalpine Ötztal Basement. Mineralogy and Petrology **43**, 237–254.

Summary

Metabasites of the southern Ötztal basement hitherto mapped as amphibolites, were identified as eclogites. Primary mineral parageneses are tschermakitic to pargasitic green amphiboles, omphacite (Jd_{40}), garnet II ($Gr_{20\text{-}30}Py_{10}$), phengite ($Si_{3.5}$), zoisite, rutile and quartz. Al-pargasite (ca. 20 wt% Al_2O_3) rims between garnet and omphacite are interpreted as retrograde reaction products.

Retrogression of the eclogitic parageneses reflecting decreasing pressure and increasing temperature conditions are: Symplectites of diopside and plagioclase after omphacite, Al- and Na-poor green amphiboles, grossularite-poor garnet III surrounding garnet II partly with atoll textures and symplectites of biotite and plagioclase replacing phengite. Continuation of retrogression with decreasing temperature conditions is indicated by actinolitic amphiboles and albite-rims between amphibole II and quartz.

A pre-eclogitic metamorphic stage is only recorded by discontinuous garnet I cores of grossular-poor composition. Minimum pressure and temperature conditions of the eclogite stage derived from Jd-content of omphacite and the gt-cpx-geothermometer are 1–12 kbar and 500-550°C. Maximum temperature conditions of the posteclogitic stage were between 600 and 650°C. The presence of these eclogitic metabasites as lenticular interlayers within ortho- and paragneisses indicates high pressure metamorphic conditions within the entire rock-sequence. This interpretation is confirmed by the occurrence of phengite-rich micas in orthogneisses indicating pressures of approx. 11 kbar. Secondary chemical changes of these phengites to muscovite-rich compositions again show the decreasing pressure conditions in the southern Ötztal basement after the eclogite stage. The age of the eclogite stage is interpreted as Eo-Alpine due to the following arguments:

The eclogites show concordant, tectonically undisturbed contacts to the encasing orthogneiss-metapelite series. This points to a common history during the last metamorphic stage.

Continuous readjustment from high to intermediate pressure conditions is observed in both eclogites and the acid country rocks.

Isotopic results from the wider study area exclusively yield Cretaceous mineral ages. Rb-Sr data on eclogite phengites (texturally clearly correlated with the high-P stage) and thin whole rock slabs of layered eclogites are in agreement with a dominant post-Variscan crystallization history, following a continuous high-P/low-T to low-P/high-T loop.

Field relations and petrography

At the southeastern corner of the zone of high-Alpine metamorphic overprint (Alpine staurolite zone ASZ), eclogitic rocks are exposed in a number of outcrops. (Hoinkes & Thöni 1987; Fig. 1). These rocks form s-parallel layers and lenses within acid gneisses and micaschists. A within-plate basaltic origin for equivalent amphibolite occurrences from the wider study area was postulated by Poli (1989).

Eclogites/amphibolites and enclosing metapelites show concordant and planar contacts indicating a coherent rock sequence. Eclogites form massive dark lay-

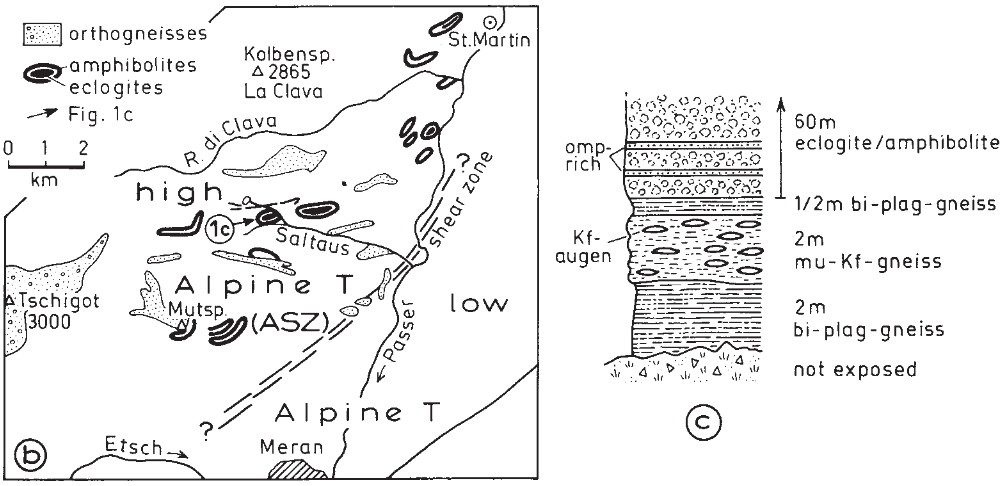

Fig. 1. (b) Simplified map of part of the southeastern ASZ in the southern Ötztal basement showing the outcrops of eclogitic rocks (full black). (c) Sketch of the undisturbed contact of eclogite and country rocks gneisses at Untere Stieralm (Saltaus valley)

ers of dm- to m-thickness within garnet-amphibolites. A continuous transition from eclogite in the center of the layers to amphibolite at the layer-margins can be observed. The eclogites are typically banded on a mm- to cm-scale with alternating light green pyroxene-rich and dark green amphibolite-rich layers. The main foliation is parallel to this compositional layering.

Mineralogy

Eclogites with little retrogressive overprint mainly show a four phase assemblage
clinopyroxene (omp) + garnet (gt) + green amphibole (amp) + quartz (qu)

Additional primary phases that may be present in various amounts are phengitic muscovite (mus), zoisite (zo), rutile (rt) and ilmenite (il). Textures indicating the stable coexistence of this four phase assemblage are (1) straight grain boundaries and 120° triple grain boundaries in quartz-rich domains (2) inclusions of clinopyroxene, garnet and amphibole within each other. Three generations of garnets can be distinguished based on composition and textures:

garnet I: chemically distinct cores within garnet II; rare
garnet II: major gt population; idioblastic grains with inclusions of qu, omp, amp, zo, qu
garnet III: atoll garnets as overgrowths on the eclogitic fabric; post eclogite stage

Primary eclogitic amphiboles are greenish and occur as dominant matrix minerals in textural equilibrium with omp and gt II. Bluish amphibole may be present as reaction rims between garnet II and omphacite or its symplectites and are therefore younger than gt II, omp and primary amphiboles but older than the symplectites.

Retrogressive alteration is indicated by the following textures:

(1) extremely fine-grained felty symplectites surrounding omp. The symplectites consist of diopside + plagioclase $\pm$ amphibole
(2) symplectites of greenish amphibole + plagioclase around primary green amphiboles
(3) albite-rims along quartz-amphibole grain boundaries
(4) myrmecitic symplectites of biotite + plagioclase surrounding phengites. Symplectite formation may lead to total replacement of phengites by coarse biotite + plagioclase intergrowths. These indicate the former presence of an eclogitic assemblage even in case the latter was totally obliterated by retrogression

Mineral chemistry

Clinopyroxene

Primary omphacites are moderately zoned with Jd41-35 in the cores and Jd35-30 at the rims. Secondary symplectitic clinopyroxenes are diopside-rich with only 2-12 mol% Jd-component.

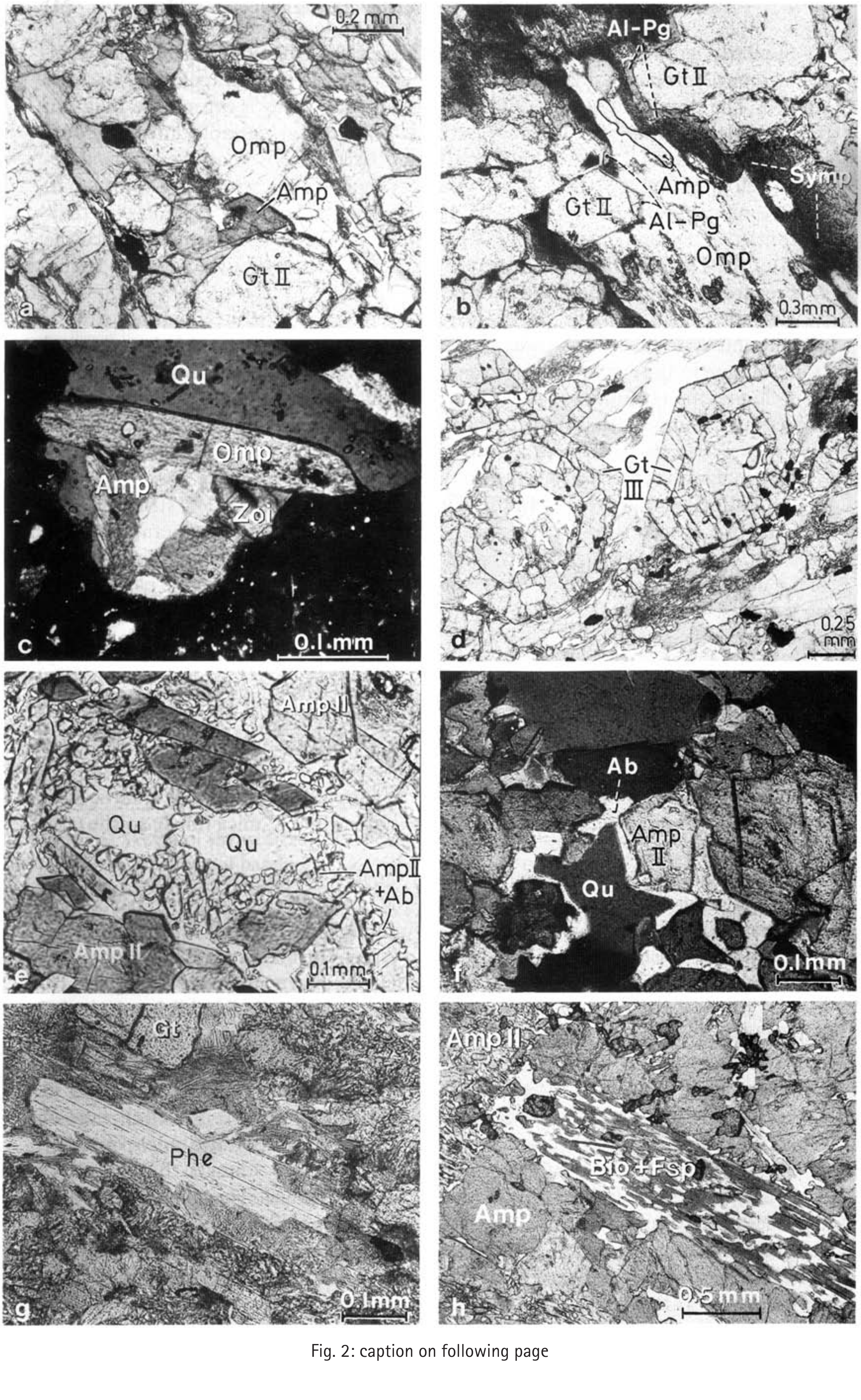

Fig. 2: caption on following page

Fig. 2: **(a)** Equilibrium textures between omp, amp and gt II; **(b)** omp with amp-inclusions and symplectite rim; bluish Al-pargasite is present as rim between gt II and omp/symplectite; **(c)** eclogite assemblage omp + amp + zoi + qu as inclusion in gt II; **(d)** post-eclogitic atoll garnets (gt III); **(e)** post-eclogitic amphibole (amp II) in a matrix of cogenetic plagioclase; **(f)** albite rims between amp II and qu; **(g)** fine-grained corona of biotite + plagioclase surrounding phengitic muscovite; **(h)** biotite + feldspar pseudomorph after phengitic muscovite

Garnet

The various garnet generations have the following chemical characteristics:

garnet I: homogeneous cores in garnet II rich in Fe and Mg and poor in Ca rel. to garnet II (Fig. 3)

garnet II: $Py_{10-20}Gro_{20-30}Alm+Spe_{50-60}$; weak zoning with increasing Mg and Fe and decreasing Ca towards the rims (Fig 3)

garnet III: lower in Ca and higher in Fe and Mg rel. to garnet II (Fig. 3)

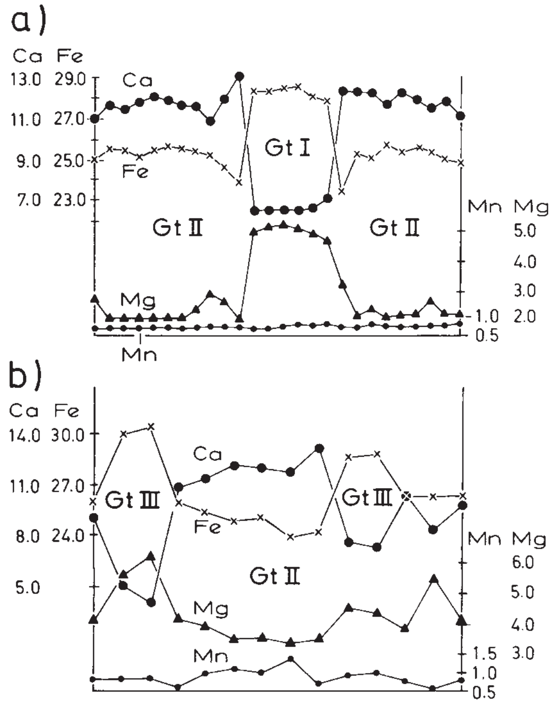

Fig. 3: (a) discontinuously zoned garnet with gt I in the core and overgrowth of gt II; profile length 0.3 mm; numbers are wt% oxides; (b) discont-inuously zoned garnet with gt II in the core and asym-metric overgrowth of atoll garnet gt III; profile length 1.0 mm

Amphiboles

primary greenish amphiboles are rich in Na and poor in Ca with tschermakitic to pargasitic composition. A core-to-rim zoning towards Na-poor pargasite or actinolite may be present. Likewise, secondary symplectitic amphiboles are Al-poor with actinolitic compositions. The bluish amphibole rims between omp and gt may reach 20 wt% Al_2O_3 and can be classified as Al-pargasites. Their formation can be ascribed to a reaction

omp + gt + H_2O = amp + $Mg_{-1}Si_{-1}Al_2$

which proceeds after the climax of the high-P event but prior to the retrogression of omphacite.

Geothermobarometry

Temperatures

Temperatures calculated from Fe-Mg exchange of coexisting gt II and omp yield temperatures of 545 ± 15°C and 496 ± 15°C based on the calibrations of Ellis & Green (1979) and Krogh (1988) respectively. Pairs of atoll garnet rims and symplectitic diopsides – not in textural equilibrium – yield temperatures of around 630°C.

Pressures

Minimum pressures for the eclogite stage based on the jadeite contents of clinopyroxene in equilibrium with quartz are 11–12 kbar for omp cores and 9-10 kbars for omp rims. Symplectitic diopsides yield pressures of 5–6 kbar for the retrogressive event. These results are in agreement with pressures derived from phengite barometry (Fig. 4).

Isotopic results

Rb-Sr isochron ages show a rather large scatter ranging from 143 ± 2 (2s) Ma to 71 ± 2.5 Ma. The oldest age was derived from the least altered of the investigated eclogite samples (T1302). Sr and Sm isotopic signatures $^{87}Sr/^{86}Sr$ = 0.70534 ± 4, $^{143}Nd/^{144}Nd$ = 0.51291 ± 2) from the same sample characterize this rock as part of an old (pre-alpine) continental basalt province that has undergone polymetamorphic evolution. The young age of 71 ± 2.5 Ma was obtained from a strongly retrogressed eclogite and is similar to an age of 77 ± 3 Ma obtained from white mica of a gneiss in the immediate vicinity (Fig. 5). The latter two ages fit into the Eo-Alpine

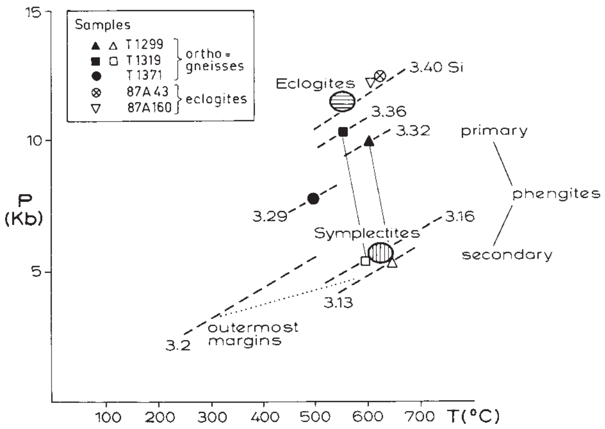

Fig. 4: Phengite barometry for orthogneisses (T1299 = eclogite country rock, T1319 and T1371 from ASZ but not related to eclogites) and eclogites (87A43, 87A160). Temperatures were derived by gt-bio thermometry in adjacent metapelites. Numbers refer to Si per 11 (O, OH) in the phengite formula. Also shown are minimum P-conditions for eclogite formation (horizontally hatched field) and the symplectite stage (vertically hatched field)

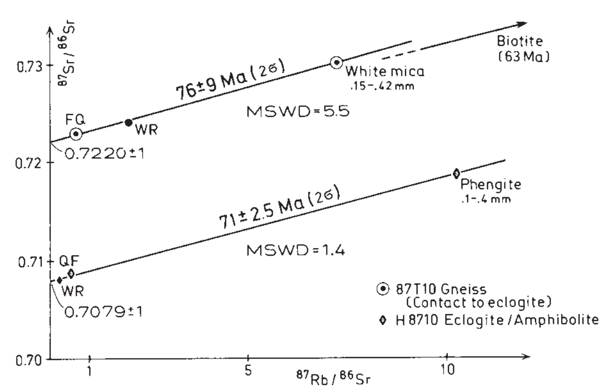

Fig. 5: Mineral isochrons for eclogite amphibolite and enclosing gneiss at Untere Stieralm

group of ages measured within the ASZ (Thöni 1988).

Conclusions

- Protoliths of the eclogites of the southern ÖSCC are old continental (within plate) basalts that underwent polymetamorphic evolution during both pre-alpine (Variscian) and alpine periods of metamorphism
- Petrologic, isotopic data and field relations favor an Eo-Alpine age of the eclogites in the southern ÖSCC and indicate a common history of eclogites and their host rocks since the time of the first penetrative deformation
- The only relics of pre-alpine metamorphism are cores of discontinually zoned garnets indicating temperatures > 600°C for this pre-alpine event.
- The Alpine P-T path of the eclogites is characterized by
  - *pressure peak*: ≥ 12 kbar at temperatures of 500-550°C (eclogite facies)
    assemblage of eclogites: garnet + omphacite + phengite + amphibole
    phengites in country rocks: Si = 3.32–3.36 apfu
    timing of pressure peak: around 140 Ma
  - *temperature peak*: *600-630°C at pressures of 5–7 kbar* (amphibolite facies)
    assemblage of eclogites: garnet + symplectite + plagioclase + amphibole
    phengites in country rocks: 3.13 – 3.16 apfu
    timing of temperature peak: around 90 Ma
  - *retrogressive stage*: T ≤ 300°C, P < 5 kbar (greenschist facies)
    assemblage: actinolite (rims around primary amphibole)
    phengites in country rocks: 3.2 apfu
    timing of retrogression: around 65 Ma
- The assumption of alpine high pressure conditions in the southern ÖSCC is consistent with Eo-Alpine P-T conditions of 8-10 kbar at around 600°C in the Schneeberg Complex immediately N of the eclogites

References

Ellis, D.J. & Green, D.H., 1979. An experimental study of the effect of Ca upon garnet-clinopyroxene Fe-Mg exchange equilibria. Contributions to Mineralogy and Petrology **71**, 13–22.

Hoinkes, G. & Thöni, M., 1987. New findings of eclogites within the eoalpine amphibolite grade area of the Ötztal basement. Terra Cognita **7**, 96.

Krogh, E.J., 1988. The garnet-clinopyroxene Fe-Mg geothermometer – a reinterpretation of existing experimental data. Contributions to Mineralogy and Petrology **99**, 44–48.

Poli, S., (1989a). Pre-hercynian Magmatism in the Eastern Alps: the origin of metabasites from the Austroalpine basement. Schweizerische Mineralogische und Petrographische Mitteilungen **69**, 407–421.

Thöni, M., 1988. Rb-Sr isotopic resetting in mylonites and pseudotachylites: implications for the detachment and thrusting of the Austroalpine Basement nappes in the Eastern Alps. Jahrbuch der geologischen Bundesanstalt **131/1**, 169–201.

Stop No. 5: Paragonite-bearing amphibolitesand garbenschists of the central Schneeberg Complex

Locality: Seewertal; 750–1000 m E of Seewersee (2056 m); start of track at an altitude of 2020 m from Timmelsjoch road direction obere Glanegg Alm

From: Konzett, J. & Hoinkes, G. (1996) Paragonite - hornblende assemblages and their petrologic significance: An example from the Austroalpine Schneeberg Complex, Southern Tyrol, Italy. Journal of Metamorphic Geology **14**, 85–101.

Summary

Paragonite-bearing amphibolites occur interbedded with a garbenschist-micaschist sequence in the Austroalpine Schneeberg Complex, southern Tyrol. The mineral assemblage mainly comprises paragonite + Mg-hornblende/tschermakite + quartz + plagioclase + biotite + ankerite + Ti-phase ± garnet ± muscovite. Equilibrium PT-conditions for this assemblage are 550-600°C and 8-10 kbar estimated from garnet-amphibole-plagioclase-ilmentite-rutile and Si-contents of phengitic muscovites. In the vicinity of amphibole paragonite is replaced by symplectitic chlorite + plagioclase + margarite ± biotite assemblages. Muscovite in the vicinity of amphibole reacts to form plagioclase + biotite + margarite symplectites The reaction of white mica + hornblende is the result of decompression during uplift of the Schneeberg Complex. The breakdown of paragonite + hornblende is a water-consuming reaction and therefore it is controlled by the availability of fluid on the retrogressive PT-path. Paragonite + hornblende is a high-temperature equivalent of the common blueschist-assemblage paragonite + glaucophane and represents restricted PT-conditions just below omphacite stability in a mafic bulk system. While paragonite + glaucophane breakdown to chlorite + albite marks the blueschist/greenschist transition, the paragonite + hornblende breakdown observed in Schneeberg Complex-rocks is indicative of a transition from epidote-amphibolite-facies to greenschist-facies conditions at a flatter PT-gradient of the metamorphic path compared to subduction-zone environments. Ar/Ar-dating of paragonite yields an age of 84.5±1 Ma corroborating an Eo-Alpine high pressure metamorphic event within the Austro-alpine unit west of the Tauern Window.

Sample Petrography

The paragonite + hornblende bearing rocks occur at a single outcrop as a ca. 3 m thick layer in a sequence of extremely coarse-grained, amphibole bearing calc-micaschists with garben-textures. Within this layer coarse-grained massive textures lacking any foliation predominate. The distinctive appearance of these paragonite amphibolites is due to radiating silvery platelets of paragonite reaching up to 5 mm in diameter. Some dm-wide layers of a fine-grained variety of this rock type lacking macroscopic paragonite occur intercalated with the massive paragonite amphibolites. These fine-grained layers are in part well foliated. Microscopic examination reveals hornblende, paragonite, quartz and plagioclase to be major constituents of all paragonite amphibolites, together making up about ca. 70 vol.% of the rock (Fig. 1c). The most striking microscopic feature is the bowtie shape of the paragonites and their symplectitic replacement (Fig. 1a, c). In one sample muscovite occurs as additional white mica forming isolated laths or intergrowths with paragonite; it can be distinguished from the latter by the lack of radiating textures. Muscovites, too, show replacement textures (Fig. 1d) which will be described below in more detail. Hornblende forms poikiloblastic prisms up to 10 mm in length. Both paragonite and hornblende contain many inclusions of all matrix phases except garnet, chlorite, cummingtonite and talc. Garnet occurs as euhedral crystals up to 5 mm in size and contains the same inclusion suite as paragonite and hornblende. Ankerite and calcite occur as a minor constituents. While ankerite forms blocky, isolated crystals, calcite and associated chlorite replace the amphibole. Actinolite was also observed as optically discontinuous rims around hornblende grains. Talc is present in one sample as small rims around

Table 1. Assemblages and estimated modal compositions of paragonite amphibolites

sample No.	173/1	601/1	601/3	601/4	610/2	613	614	162	165	169
Quartz	•	•	•	•	•	•	•	x	x	x
Plagioclase	•	•	•	x	•	x	•	•	•	•
Ca-Amphibole	x	x	x	x	x	x	x	x	x	x
Paragonite	•	+	•	•	•	•	•	+	+	+
Muscovite	--	--	--	--	•	--	--	--	--	--
Biotite	+	+	•	•	+	•	+	+	•	+
Clinozoisite	•	•	•	•	•	•	•	+	+	+
Garnet	•	•	•	+	•	--	•	•	•	+
Ankerite	•	•	+	+	+	+	+	+	•	•
Calcite	+	+	+	--	+	--	+	--	--	+
Rutile	+	+	+	+	+	+	+	+	+	+
Ilmenite	+	+	+	+	+	+	+	+	+	+
Titanite	--	+	--	--	--	--	+	--	--	--
Tourmaline	--	--	--	--	--	--	+	--	--	--
Symplectite*	•	•	•	•	•	•	•	•	•	+
Cummingtonite	+	--	--	--	--	--	+	--	--	+
Actinolite	--	--	--	--	--	--	+	--	--	+
Talc	--	--	--	--	--	--	--	--	--	+

*) Plag + Margarite ± Chlorite ± Biotite; x > 20 vol%; • 2-20 vol%; + < 2 vol%; - absent

Table 1: Assemblages and estimated modal compositions of paragonite amphibolites

quartz grains associated with ankerite and fine grained calcite. Ti-phases in the matrix and within the outer zones of garnets are rutile and ilmenite occurring as intergrowths and as separate grains. Titanite exclusively occurs as inclusions in hornblende and garnet, and within garnets it is confined to the centers where it partly reacts to form ilmenite.

White mica breakdown textures

Paragonite breakdown

Within the matrix, paragonite is surrounded by very fine-grained symplectitic reaction rims. Paragonite breakdown always occurs in the vicinity of hornblende, and it is only in a few cases that unaltered grain-boundaries between these two phases can be observed (Fig. 1b). Rare paragonite inclusions in hornblende and garnet or grains armoured by quartz in small quartz pods are unaltered.

Two different product assemblages can be identified:

1) plagioclase + chlorite + margarite
2) plagioclase + biotite + margarite ± chlorite

Chlorite and biotite occur as lath-shaped grains embedded in felty-looking plagioclase that can easily be distinguished from clear matrix plagioclase. With one exception (SW613) margarite can only be identified with the microprobe. Modal estimates of the symplectite phases always indicate plagioclase >> chlorite/biotite > margarite. Mineral inclusions in paragonite are not affected by the breakdown reaction. Clinozoisite „survives" breakdown of the paragonite host with no change of its modal amount. Biotite produced by paragonite breakdown can be distinguished from primary matrix biotite by its smaller grain size and its occurrence as „beards" along former paragonite - hornblende grain boundaries. Within a single thin section all stages of replacement from almost unaltered paragonite to a complete pseudomorphism can be observed. Fig. 2 shows typical textures of paragonite amphibolites.

Muscovite breakdown

Like paragonite, muscovite is surrounded by reaction rims. The breakdown assemblage is

plagioclase + biotite + margarite

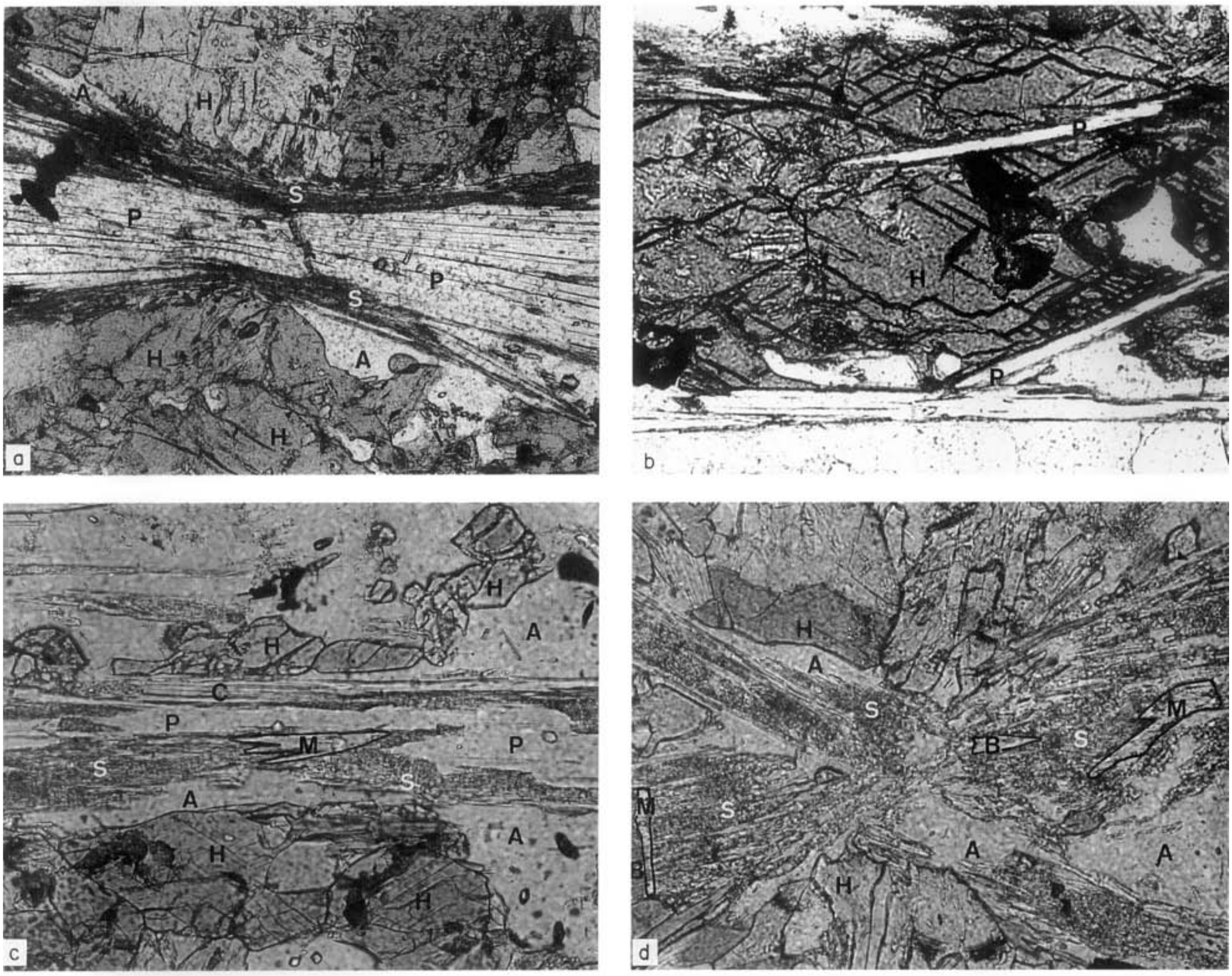

Fig. 1: Photomicrographs of typical textures of pargonite amphibolites **(a)** bow-tie paragonite showing symplectites along contacts with hornblende; edge length of image 2.5 mm; **(b)** unaltered paragonite laths included in hornblende; edge length of image 1.8 mm; **(c)** paragonite partly replaced by chlorite + plagioclase + margarite forming a fine-grained symplectite; edge length of image 0.7 mm; **(d)** muscovite laths totally replaced by biotite + plagioclase + margarite; edge length of image 0.6 mm; abbreviations: A = plagioclase; B = biotite; C = chlorite; H = hornblende; M = margarite; P = paragonite; S = symplectite

Textures of muscovite breakdown are different from those of paragonite breakdown: Plagioclase forms clear grains and margarite is coarse and can be identified under the optical microscope. While paragonite breakdown always commences at the outermost rims leaving the grain-center unaffected even in an advanced stage of alteration, muscovite decomposition also occurs in the grain interior along cleavage plains (Fig. 1d).

Mineral chemistry

Amphiboles

Primary matrix amphiboles and amphibole inclusions in garnet are Mg-hornblendes to tschermakites with Al_2O_3 contents from 12 to 18 wt%. Most of the chemical variability can be described in terms of variations in the tschermak (tk) and plagioclase (pl). (Fig. 2). Amphibole inclusions in garnet show a systematic increase in tk and pl from core to rim Secondary calcic amphiboles (actinolite and actinolitic hornblende) have low Al_2O_3 contents between 3 and 7 wt%.

White mica

Paragonite is close to end member composition with small deviations from 3.00 Si per 11 oxygens. Al contents are slightly variable and where grain-boundaries are unaltered coexisting paragonite and hornblende show a correlation in Al(IV)/Al(VI) ratios as shown in Figure 2. Margarite component of para-

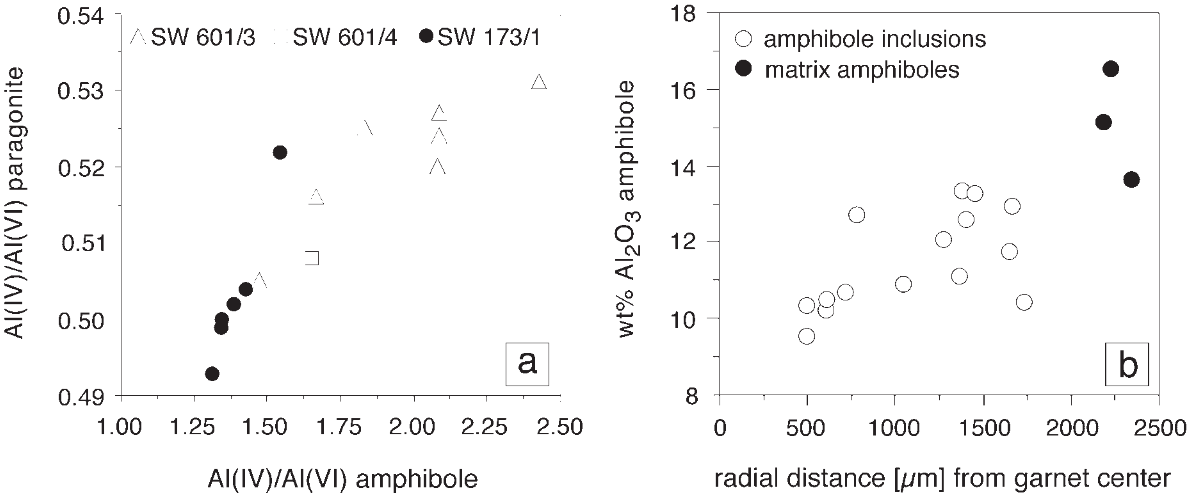

Fig. 2: **(a)** composition of coexisting calcic amphibole and paragonite rims where paragonite share unaltered grain boundaries with amphibole; **(b)** plot of wt.% Al_2O_3 of amphibole vs. radial distance from center of euhedral garnet from sample 601/1.

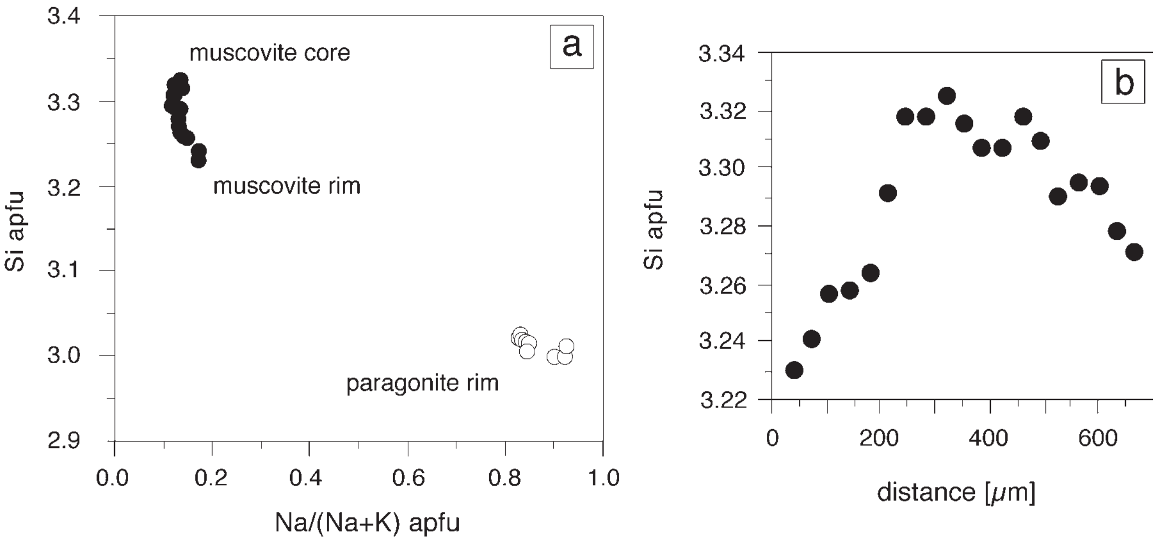

Fig. 3: (a) Composition of coexisting paragonite and muscovite in sample 610/2 in terms of paragonite and celadonite contents: (b) compositional profile of celadonite contents for the same muscovite

gonites is between 1.2 and 3.8 mol.%, muscovite component range from 3.8 to 16.9 mol.% with a maximum in the muscovite bearing sample SW 610/2. Individual paragonite grains do not show systematic compositional zoning.

Muscovite is zoned with respect to celadonite component. On the basis of 11 oxygens and Fe_{tot} = Fe^{2+}, rims have 3.23-3.25 Si pfu, and towards the core a continuous increase to 3.30–3.32 Si pfu can be observed along with a decrease in paragonite component from 12 to 17 mol.%. All analyses show a small deviation towards trioctahedral composition with 0.04–0.06 octahedral cations pfu. Figure 3 shows the composition of coexisting muscovite and paragonite.

Margarite formed during paragonite breakdown is Na-rich and shows 30–49 mol.% paragonite component. Margarite associated with muscovite breakdown has somewhat lower paragonite contents between 24 and 32 mol.%.

Biotite

Primary matrix biotites and secondary biotites formed during white mica decomposition can be

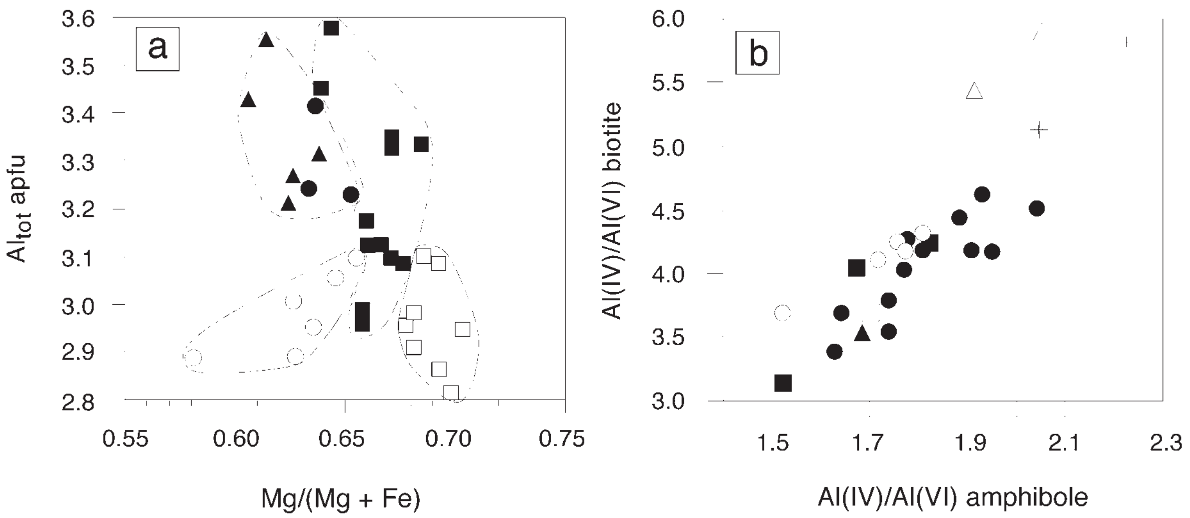

Fig. 4: **(a)** Composition of primary and secondary biotites: open circles: primary matrix biotites SW610/2; filled circles and triangles: secondary biotites formed by paragonite and muscovite breakdown SW610/2; open squares: primary matrix biotites SW601/4; filled squares: secondary biotites formed by paragonite breakdown SW601/4; **(b)** Al(IV)/Al(VI)-ratios in coexisting amphibole and biotite; filled circles: SW613; open circles SW601/1; filled triangles: SW614; open triangles: SW601/4; filled squares: SW601/3 open squares SW610/2; crosses: SW162

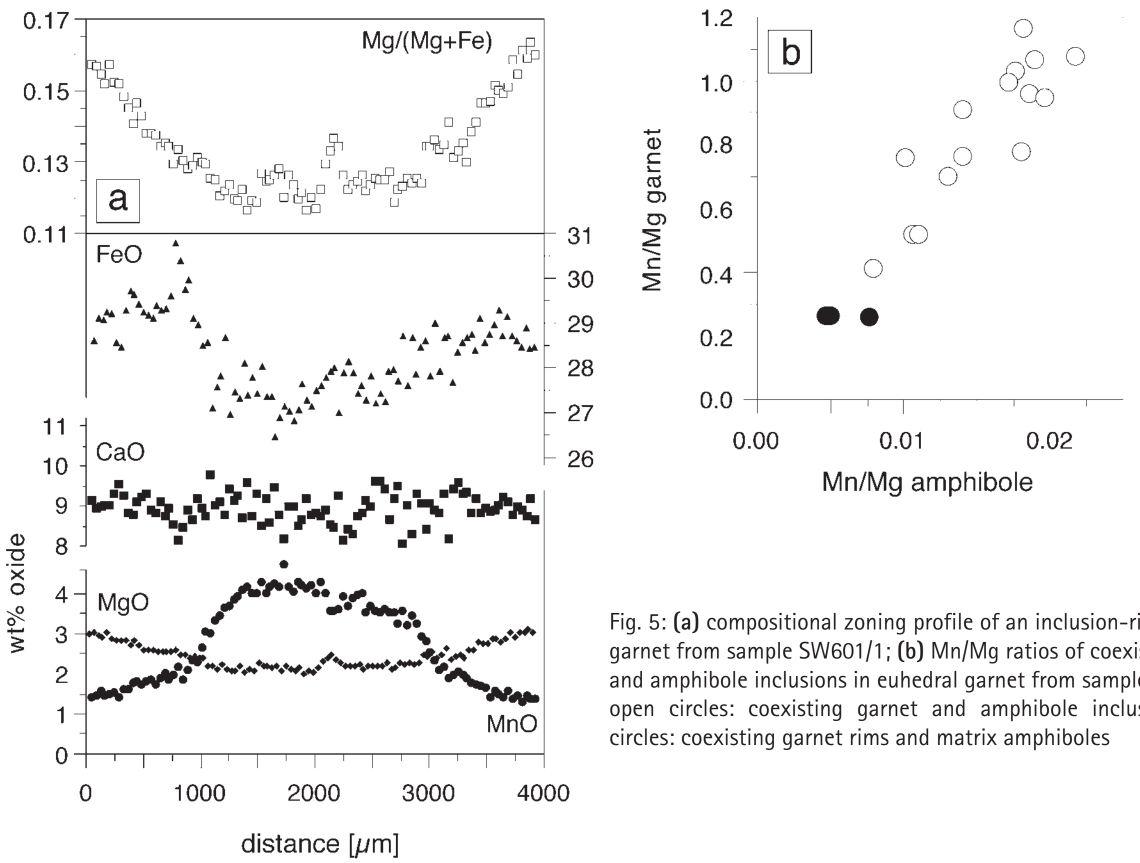

Fig. 5: **(a)** compositional zoning profile of an inclusion-rich euhedral garnet from sample SW601/1; **(b)** Mn/Mg ratios of coexisting garnet and amphibole inclusions in euhedral garnet from sample SW601/1 ; open circles: coexisting garnet and amphibole inclusions; filled circles: coexisting garnet rims and matrix amphiboles

distinguished by the higher total Al and partly by a lower X_{Mg} of secondary biotites (Fig. 4a). Primary biotites and coexisting hornblendes show a positive correlation in Al(IV)/Al(VI) ratios within individual samples as well as between different samples (Fig. 4b).

Garnet

Garnet shows bell-shaped compositional zoning with a core-to-rim increase in MgO, FeO and Mg/ (Mg+Fe) ratio and a decrease in MnO (Fig. 5a). CaO either follows the Mn-trend or, in a few cases, remains nearly constant. Garnet and coexisting amphibole inclusions show a very regular correlation in their Mn/Mg ratios (Fig. 5b). and a less pronounced correlation their Fe/Mg ratios.

Plagioclase

Primary matrix plagioclase ranges in composition from An_{18} to An_{30} with a maximum close to An_{25}. Plagioclase occurring in symplectites around paragonite is enriched in Ca with An_{35}–An_{55}. Muscovite breakdown produces plagioclase with a compositional range of An_{24}–An_{50} which overlaps that of matrix plagioclase.

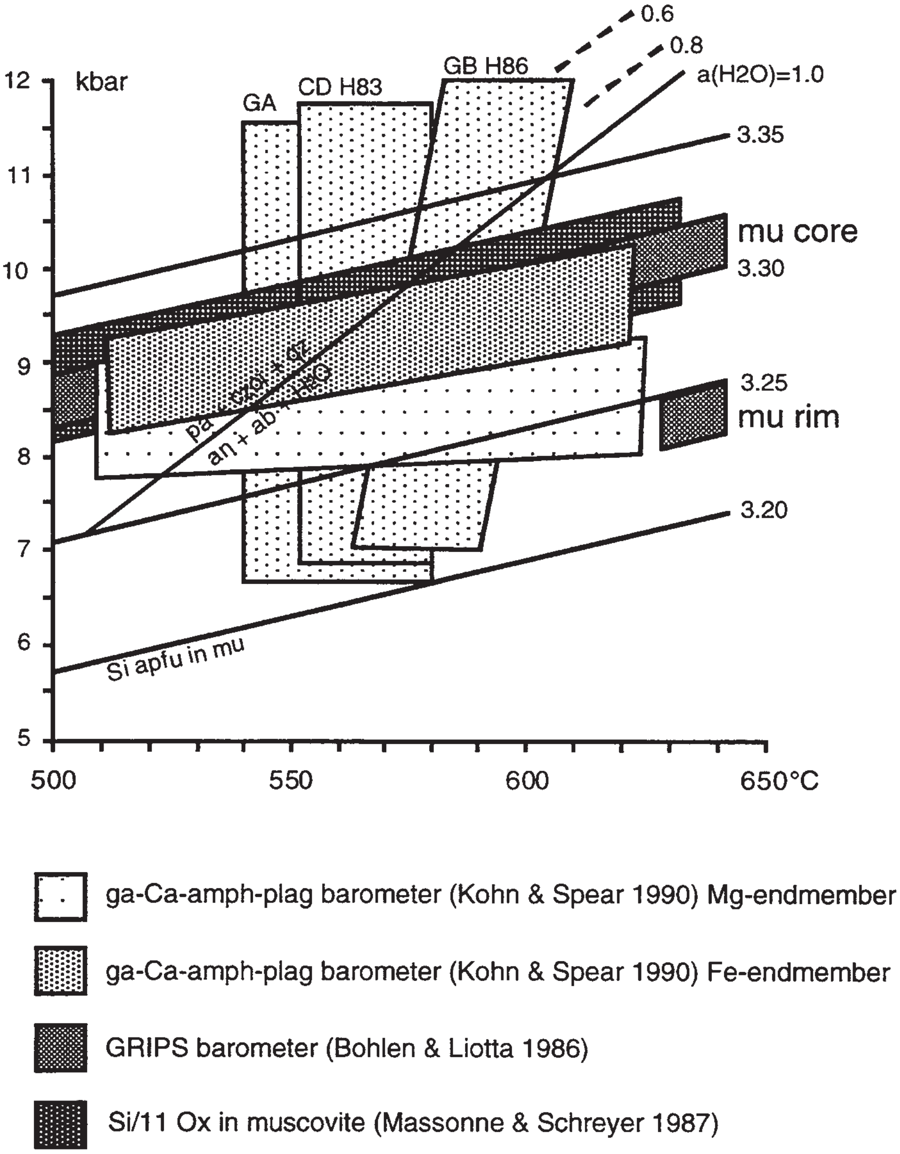

Fig. 6: P-T conditions of metamorphism derived from various geothermobarometers for paragonite amphibolites of the central Schneeberg Complex. GA: garnet-Ca-amphibole thermometer (Graham & Powell 1984); CD H83: results of calcite-dolomite thermometry (Hoinkes 1983); GB H86: results of garnet-biotite thermometry (Hoinkes 1986)

Conditions of metamorphism

Temperature

Temperatures can be derived from Fe/Mg exchange between coexisting amphibole and garnet which was empirically calibrated by Graham & Powell (1984). A mean temperature of 562 ± 21°C was obtained from 7 samples for coexisting garnet rims and amphibole rims (Fig. 6). Temperatures for amphibole inclusions in garnet (SW 601/1) are slightly lower with 541 ± 16°C. Results are in good agreement with calcite-dolomite and garnet-biotite thermometry applied to adjacent tremolite-marbles and staurolite-kyanite-micaschists by Hoinkes (1983, 1986) with mean values of 566 ± 14 and 581 ± 12°C respectively (Fig. 6).

Pressure

Minimum pressures can be derived from celadonite contents of muscovite in sample SW610/2. Muscovite cores from 610/2 have 3.30 - 3.32 Si pfu. corresponding to > 9 kbar at 600°C according to Massonne & Schreyer (1987).

Coexisting amphibole + garnet + plagioclase allow application of the empirically calibrated barometers of Kohn & Spear (1990). The resulting pressures are 8.5 ± 0.6 kbar and 9.4 ± 0.5 kbar for Mg- and Fe-endmember reactions. In addition pressures can be derived from coexisting garnet + rutile + ilmenite + plagioclase (GRIPS) based on the experimental calibration of Bohlen & Liotta (1986). The GRIPS-assemblage yields a mean pressure of 9.6 ± 0.6 kbar from 5 samples.

An additional constraint on metamorphic pressure is placed by texturally stable paragonite + clinozoisite + quartz + plagioclase. The relevant equilibrium amongst these phases is

paragonite + 2 clinozoisite + 2 quartz = 4 anorthite + albite + 2 H_2O (1)

The pressure calculated at T = 580°C and aH_2O = 1.0 with representative phase compositions and activities using the TWEEQ-software (Berman et al. 1991) is 10.0 kbar. A reduced water-activity slightly increases pressures, for example for aH_2O = 0.8 the shift is near 0.5 kbar.

The age of metamorphism

Previous studies on SC metapelites report Rb/Sr ages of ca. 90–75 Ma for muscovite and biotite (Thöni 1983, Thöni & Hoinkes 1987) corresponding to cooling after the peak of Eo-Alpine metamorphism. Textures and garnet-zoning patterns indicate a mono-metamorphic history of the SC (Hoinkes 1983). In order to constrain the timing of high P-metamorphism reported by paragonite + hornblende assemblages, a paragonite concentrate from sample SW601/3 was used for $^{40}Ar/^{39}Ar$ dating. The concentrate displays a mean plateau age of 84.5 ± 1.0 Ma for heating increments from 850–1250°C corresponding to ca. 92 % of the released gas (Fig. 7). The heating steps show little variation in apparent K/Ca ratios, indicating gas evolution from com-

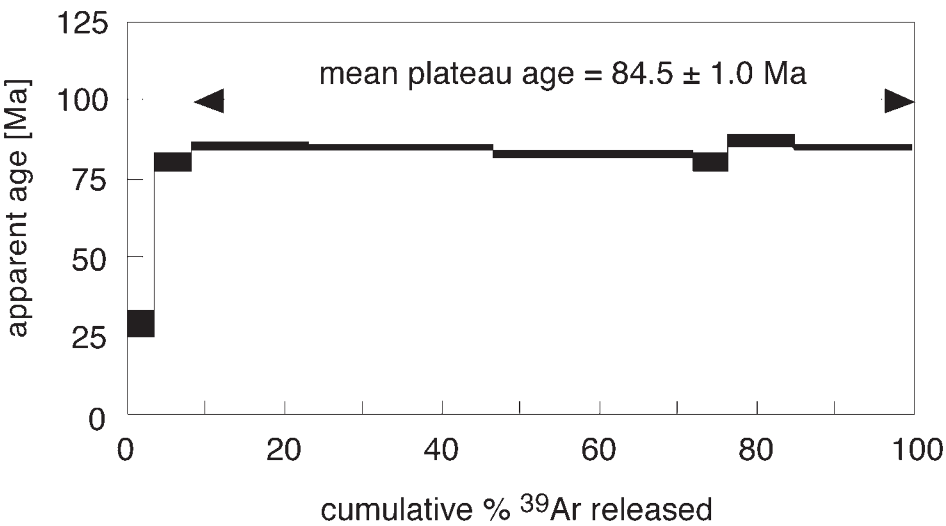

Fig. 7: Ar/Ar age of paragonite concentrate from sample SW601/3

positionally uniform populations of intracrystalline sites.

Discussion of phase relations

The high pressure stage

The stable mineral assemblage prior to symplectite-formation was

hornblende + paragonite + clinozoisite + garnet + biotite ± muscovite + ankerite + plagioclase + quartz + Ti-phase

This is concluded from both textural and mineral chemical features: paragonite and hornblende form inclusions within each other; with the exception of plagioclase all phases of the high pressure stage occur as inclusions within garnet. The correlation of Al(IV)/Al(VI) ratios in coexisting paragonite + hornblende and biotite+ hornblende indicates attainment of local exchange equilibrium between these phases.

Garnet zoning patterns with continuous decrease in MnO and increase in X_{Mg} from core to rim indicate garnet growth under increasing PT conditions. This is supported by systematic changes in amphibole inclusion chemistry and the distribution of Ti-phase inclusions: Amphibole inclusions in garnet show systematically lower values of tschermak and plagioclase exchange component than matrix amphiboles and a regular increase in Al_2O_3 with increasing distance from garnet core (Fig. 2). These features along with the Mn/Mg and Fe/Mg correlations between amphibole inclusions and host garnet support the assumption of progressive garnet and amphibole growth under conditions of local equilibrium. Occasional matrix amphibole zoning with core-to-rim increase in Al_2O_3, Na_2O, TiO_2 and K_2O also clearly indicates a progressive metamorphic evolution. (e.g. Spear 1981) Figure 8 shows invariant points in the NCMASH-system delimiting the stability-field of tschermakite + paragonite + H_2O. The relative locations of the invariant points were determined with thermodynamic data of the TWEEQU software using pure endmember compositions. According to this diagram paragonite + tschermakite can form during progade metamorphism from the typical greenschist facies assembages albite + chlorite (against arrow) or albite + chlorite + clinozoisite (with arrow).

The symplectite stage

Textures indicate two reactions which lead to the loss of paragonite:

paragonite + hornblende → plagioclase + chlorite + margarite (2a)

paragonite + hornblende → plagioclase + biotite + margarite ± chlorite (2b)

Reaction (2a) is dominant, whereas (2b) is well developed only in two samples 601/4 and 610/2. Neglecting small amounts of margarite, reaction (2a) can be idealized as

3 paragonite + 5 tschermakite + 4 H_2O = 3 clinochlore + 3 albite + 10 anorthite + quartz (3)

Replacing tschermakite by glaucophane, a reaction equivalent to (3) is

3 paragonite + 5 glaucophane + 4 H_2O = 3 clinochlore +13 albite + quartz (4)

Reaction (4) is well known from blueschists and marks the transition from blueschist to greenschist facies conditions during uplift and decompression. The similarity between reactions (3) and (4) is striking. Both have H_2O on the low-entropy side and thus can only proceed if H_2O or in general a fluid phase is available; both reactions have similar standard state properties. By analogy with reaction (4), the breakdown of paragonite + hornblende is interpreted as decompression-induced (see also Fig. 8).

The breakdown of phengitic muscovite with formation of plagioclase + biotite + quartz (+ K-feldspar) symplectites is also widespread in high pressure rocks during decompression. According to the thinsection observation, the muscovite breakdown in SW610/2 can be formulated as

muscovite + Na^+ + Ca^{2+} → biotite + plagioclase + margarite (5a)

or

muscovite + amphibole → biotite + plagioclase + margarite (5b)

The lack of unaltered muscovite-amphibole grain boundaries and the presence of an Al-rich phase like margarite in the symplectite suggest that (5b) was operative.

Neglecting minor components (e.g. Ti, Fe^{3+}, Mn, K) the paragonite breakdown which produces plagioclase + chlorite + margarite can be described in the system SiO_2-Al_2O_3-FeO-MgO-CaO-Na_2O-H_2O. Calculation of reaction coefficients for reaction (2a) involves a least squares solution of an over-determined system of equations (e.g. Giramitra & Day 1990) using idealized mineral compositions. For samples

SW173/1 and SW169 the following model reactions are obtained:

173/1 2.32 pa + 1.46 amph + 0.55 H_2O → chl + 4.77 plag + 0.33 ma + 0.67 qz (6)

169 2.51 pa + 1.45 amph + 0.68 H_2O → chl + 4.51 plag + 0.63 ma + 0.95 qz (7)

Reactions (6) and (7) agree with textural observations: H_2O is on the reactant side confirming its necessity introduction for the reaction to proceed.

The significance of the paragonite + hornblende assemblage and regional implications

Evans (1990) calculated a wedge-shaped stability field for coexisting paragonite + calcic amphibole similar to Fig. 8, denoted as epidote-amphibolite facies, separating greenschist from epidote-blueschist fields for aluminuous bulk compositions. The paragonite amphibolites presented in this study are considered an example of epidote-amphibolite facies conditions close to the eclogite facies transition in a tectonic setting of crustal thickening created by convergent movement of the African and European continental plates during the early to middle Cretaceous.

The bulk composition of SC paragonite amphibolites is comparable to average oceanic crust compositions especially with respect to Al, Mg and Na, and is similar to the bulk compositions of the eclogites (Hoinkes et al. 1991). This indicates that paragonite + hornblende stability does not require unusual bulk compositions but, on the other hand, rather restricted PT conditions: The temperature must be sufficiently high to stabilise Al-rich calcic amphibole instead of sodic or sodic-calcic amphiboles, and the pressure must be high enough to destabilise plagioclase + chlorite + quartz. In tectonic environments with steeper PT-gradients (e.g. subduction zones with PT-paths from greenschist to blueschist to eclogite facies) the equivalent assemblage would be glaucophane + paragonite . In the ÖSCC the succession is greenschist to epidote-amphibolite to eclogite facies. There is no evidence (preserved glaucophane inclusions or glaucophane pseudomorphs etc.) for crossing the blueschist-field during Eo-Alpine metamorphism in any of the rock-types investigated. The pressure range derived for SC paragonite amphibolites is supported by garbenschist-like assemblages in the vicinity containing Al-rich calcic amphibole + muscovite + kyanite ± staurolite. From his experimental work Hoschek (1990) concluded that muscovite + calcic amphibole and especially calcic amphibole + kyanite is favoured by high pressures. Selverstone et al. (1984) report a paragonite + calcic amphibole + kyanite + staurolite assemblage from the Tauern Window at 10 kbar and 550°C, they ascribe its stability to PT conditions usually not attained during regional metamorphism.

Textural observations and derivation of reaction stoichiometry show that preservation of the paragonite + hornblende assemblage is critically dependent on the availability of fluid and the degree to which fluid can penetrate the rock, the latter being controlled by grain size and deformation: the least retrogressed paragonite amphibolites are coarse-grained and show massive textures while the strongly retrogressed varieties are fine-grained and/or foliated. The survival of high-P assemblages due to limited fluid access is widespread and well documented in the Western Alps.

The breakdown of paragonite + hornblende, even if it takes place „irreversibly", i.e. is overstepped, is only possible where fluid can access the rock. Thus, calculation of the PT-conditions of paragonite + hornblende breakdown assuming equilibrium may be grossly misleading. A likely fluid source is dehydration in adjacent metapelites or the paragonite + hornblende reaction may be triggered by fluid released from preceeding muscovite breakdown which, at the same time, can supply K required for biotite formation in paragonite-symplectites.

Conclusions

- Paragonite + hornblende is an equilibrium assemblage representing rather restricted PT-conditions within the epidote-amphibolite facies in a mafic bulk system.

- Paragonite amphibolites are indicators of high pressure regional metamorphism close to, but still below omphacite stability. They must be considered direct precursors of low pressure-high temperature eclogites in a regional metamorphic regime. Pressures derived at a maximum temperature of ~600°C are 8–10 kbar.

- Ar/Ar-dating of paragonite yields an Eo-Alpine plateau age of 84.5 ± 1.0 Ma indicating a thermal climax of Eo-Alpine metamorphism around 100–95 Ma.

Fig. 8: Invariant points in the system NCMASH delimiting the stability field of paragonite + tschermakite; bold arrows indicate a suggestes P-t evolution path during Eo-Alpine metamorphism.
Abbreviations: pa = paragonite, tsch = tschermakite, ab = albite, an = anorthite, czoi = clinozoisite, chl = chlorite, py = pyrope, qz = quartz, w = water

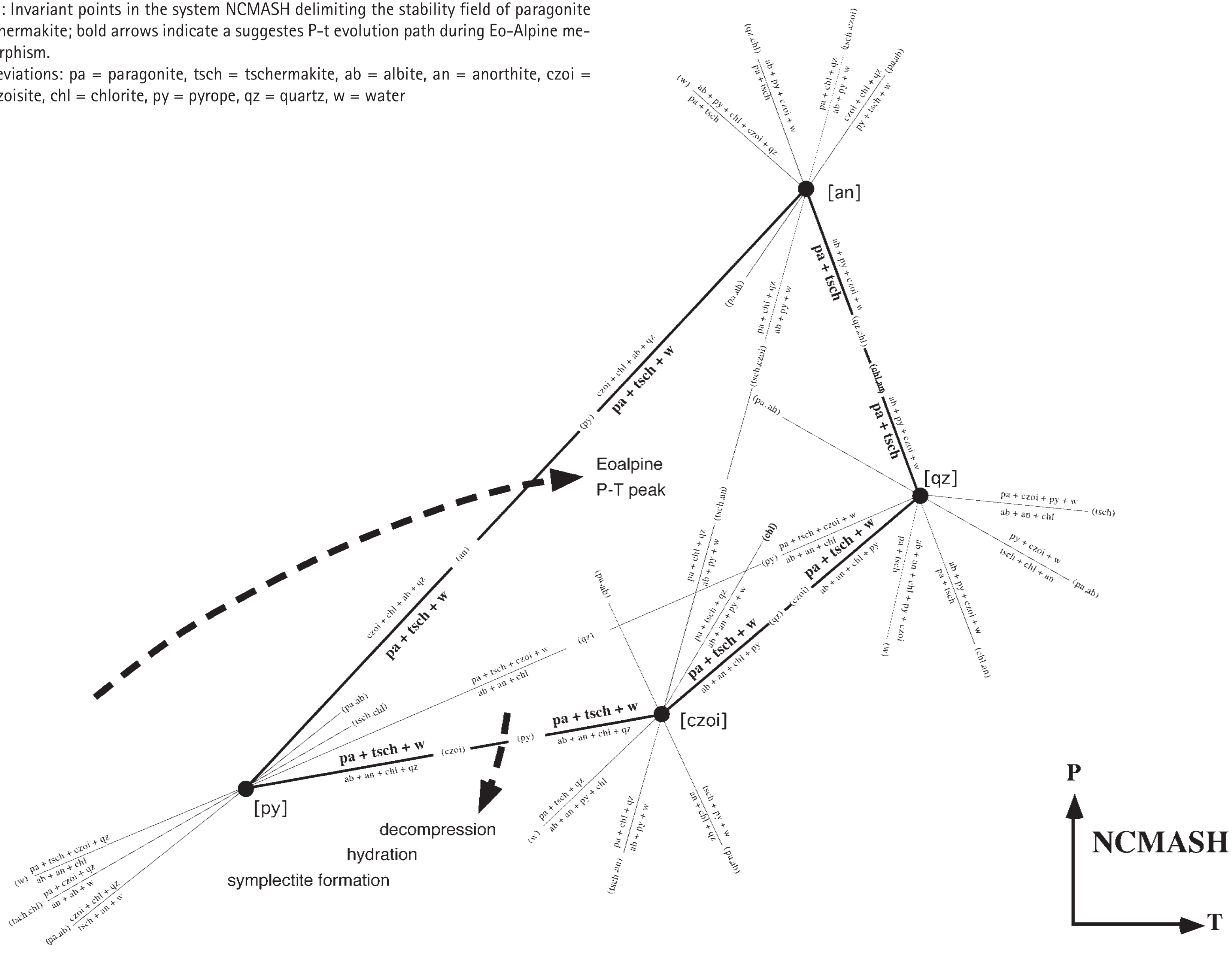

- Breakdown of paragonite + hornblende to form the greenschist facies assemblage chlorite + plagioclase + margarite ± biotite occurs during uplift and decompression of the Schneeberg Complex rocks after the peak of Eo-Alpine metamorphism. It is considered a high temperature equivalent of paragonite + glaucophane breakdown which indicates the blueschist-greenschist facies transition in high pressure regimes. By analogy, paragonite + glaucophane-bearing rocks are precursors of low temperature-high pressure eclogites in subduction zones. Reaction of phengitic muscovite to plagioclase + biotite + margarite is ascribed to the same process but may not have occured contemporaneously.
- The occurrence of high pressure metamorphism in the Schneeberg Complex is thought to be related to eclogite formation in the Ötztal-Stubai Crystalline Basement southeast of the Schneeberg Complex and strongly supports the assumption of an Eo-Alpine age of these eclogites (Hoinkes et al. 1991).

References

Berman, R. G., 1991. Thermobarometry using multi-equilibrium calculations: a new technique, with petrological applications. Canadian Mineralogist, **29**, 833–855.

Bohlen, S. R. & Liotta, J. J., 1986. A Barometer for Garnet Amphibolites and Garnet Granulites. Journal of Petrology, **27**, 1025–1034.

Evans, B. W., 1990. Phase relations of epidote-blueschists. Lithos, **25**, 3-23.

Giaramitra, M. J. & Ray, H. W., 1991. Buffering in the assemblage staurolite-aluminium silicate-biotite-garnet-chlorite. Journal of Metamorphic Geology, **9**, 363–378.

Graham, C. M. & Powell, R., 1984. A garnet-hornblende geothermometer: calibration, testing and application to the Pelona Schist, Southern California. Journal of Metamorphic Geology, **2**, 13–31.

Hoinkes, G., 1983. Cretaceous metamorphism of metacarbonates in the Austroalpine Schneeberg complex, Tirol. Schweizerische Mineralogische und Petrographische Mitteilungen, **63**, 95–114.

Hoinkes, G., 1986. Effect of grossular-content in garnet on the partitioning of Fe and Mg between garnet and biotite. An empirical investigation on staurolite-zone samples from the Austroalpine Schneeberg Complex. Contributions to Mineralogy and Petrology, **92**, 393–399.

Hoinkes, G., Kostner, A. & Thöni, M., 1991. Petrologic Constraints for Eo-Alpine Eclogite Facies Metamorphism in the Austroalpine Ötztal Basement. Mineralogy and Petrology, **43**, 237–254.

Hoschek, G., 1990. Melting and subsolidus reactions in the system K_2O-CaO-MgO-Al_2O_3-SiO_2-H_2O, experiments and petrologic applications. Contributions to Mineralogy and Petrology, 105, 393–402.

Massonne, H-J. & Schreyer, W., 1987. Phengite geobarometry based on the limiting assemblage with K-feldspar, phlogopite, and quartz. Contributions to Mineralogy and Petrology, **96**, 212–224.

Kohn, M. J. & Spear, F. S., 1990. Two new geobarometers for garnet amphibolites, with applications to southeastern Vermont. American Mineralogist, **75**, 89–96.

Selverstone, J., Spear, F. S., Franz, G. & Morteani, G., 1984. High-Pressure Metamorphism in the SW Tauern Window, Austria: P-T Paths from Hornblende - Kyanite - Staurolite Schists. Journal of Petrology, **25**, 501–531.

Spear, F. S., 1981. An experimental study of hornblende stability and compositional variability in amphibolite. American Journal of Science, **281**, 697–734.

Thöni, M., 1983. The thermal climax of the early Alpine metamorphism in the Austroalpine thrust sheet. Memorie di Science Geologiche, **36**, 211–238.

Thöni, M. & Hoinkes, G., 1987. The Southern Ötztal Basement: Geochronological and Petrological Consequences of Eo-Alpine Metamorphic Overprinting. In: Geodynamics of the Eastern Alps (eds. Flügel, H. W. & Faupl. P.), pp. 379–406, Franz Deuticke, Vienna.

Authors' addresses:
Dr. Jürgen Konzett, Dr. Peter Tropper, Institut für Mineralogie und Petrographie, Universität Innsbruck, Innrain 52, 6020 Innsbruck
Univ.-Prof. Dr. Georg Hoinkes, Institut für Mineralogie und Petrologie, Universität Graz, Universitätsplatz 2/II, 8010 Graz
e-mail:
Juergen.Konzett@uibk.ac.at
Peter.Tropper@uibk.ac.at
georg.hoinkes@kfunigraz.ac.at